

Ultralight self-interacting scalar field dark matter

Raquel Galazo-García

Collaborators: Eric Jullo, Marceau Limousin, Emmanuel Nezri

Laboratoire d'Astrophysique de Marseille

News from the dark

Marseille, November 13, 2024

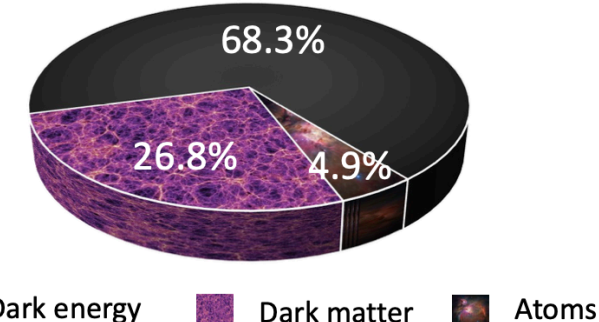


What we know about dark matter

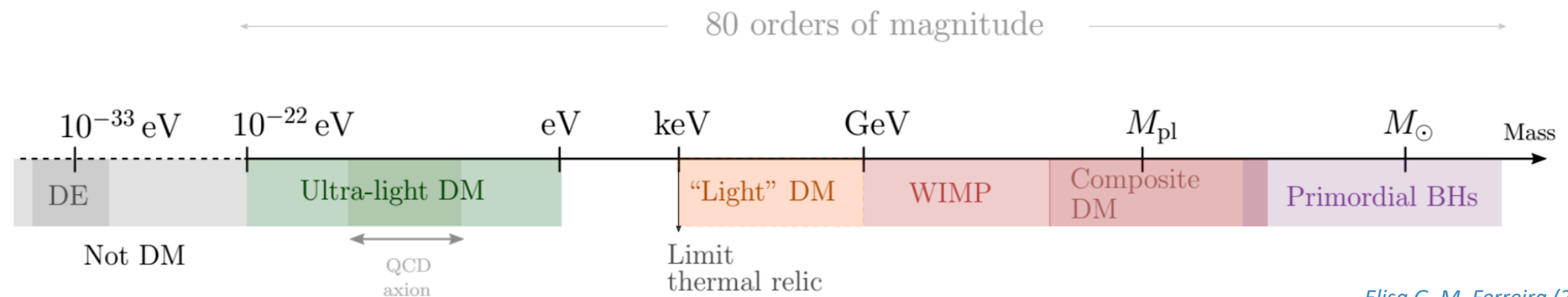
The standard cosmological model, Λ CDM → DM is described as a cold DM fluid.

- 27% of the energy density of the universe.
- Dark (transparent): no/weakly electromagnetic interactions.
- Collisionless: no/weakly self-interaction or interaction with baryons
- Cold (non-relativistic): moves much slower than c.
- Pressureless: gravitational attractive, clusters.

Energy content of the Universe



However, we remain ignorant about its basic properties for example the mass.



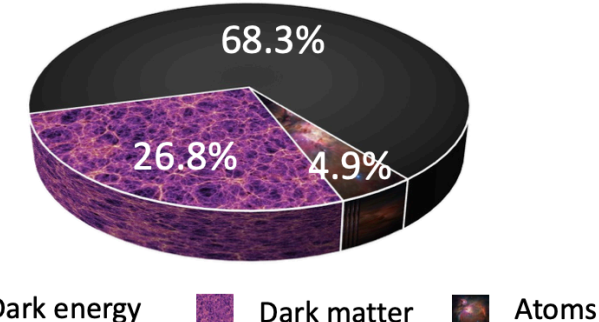
Elisa G. M. Ferreira (2020)

What we know about dark matter

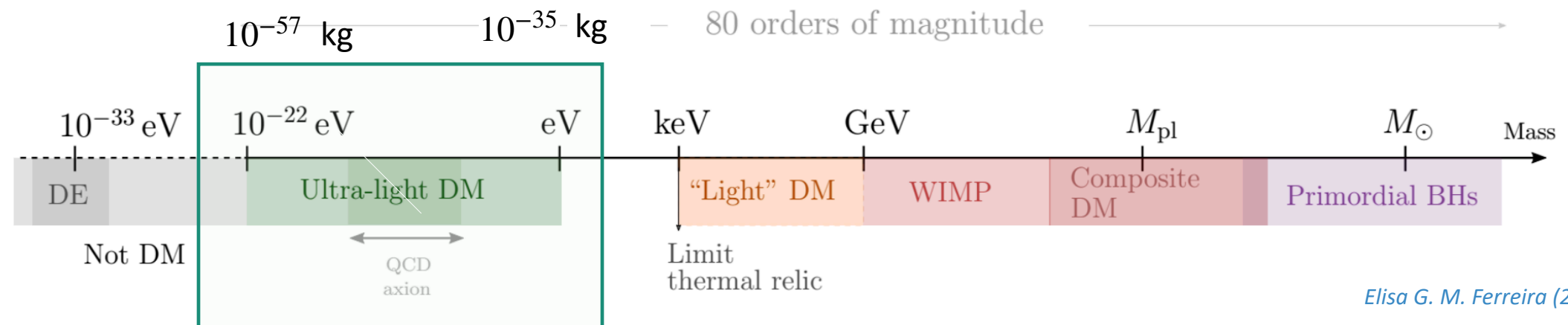
The standard cosmological model, Λ CDM → DM is described as a cold DM fluid.

- 27% of the energy density of the universe.
- Dark (transparent): no/weakly electromagnetic interactions
- Collisionless: no/weakly self-interaction or interaction with baryons
- Cold (non-relativistic): moves much slower than c.
- Pressureless: gravitational attractive, clusters.

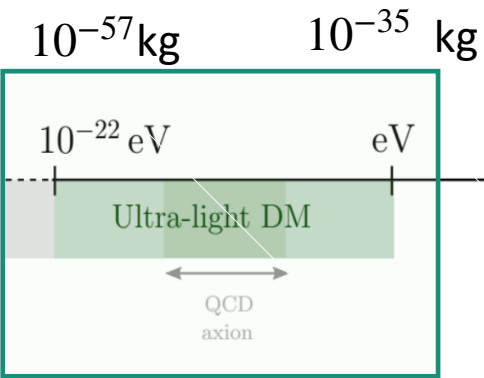
Energy content of the Universe



However, we remain ignorant about its basic properties for example the mass.

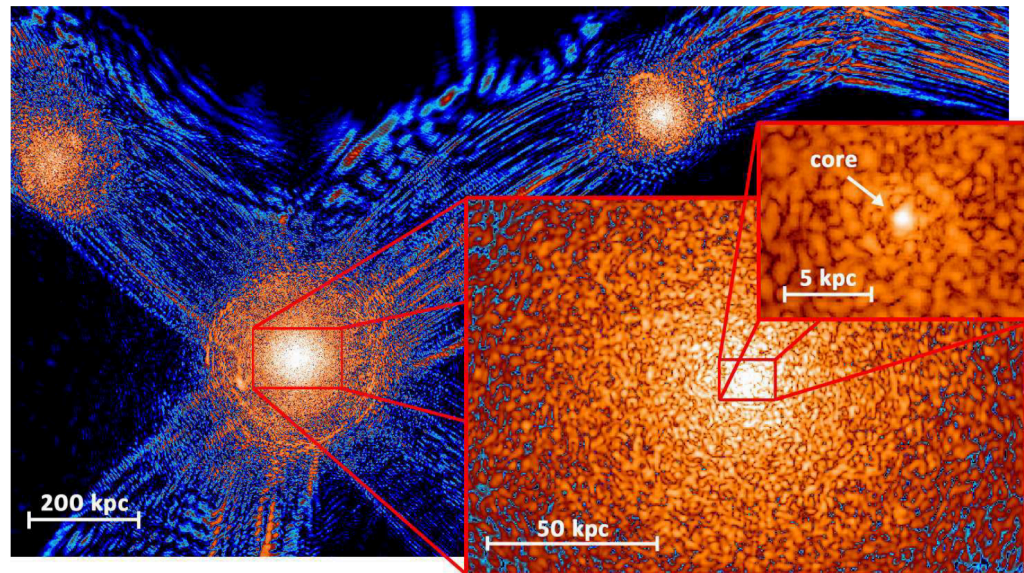


Scalar Field Dark Matter (SFDM) at small scales



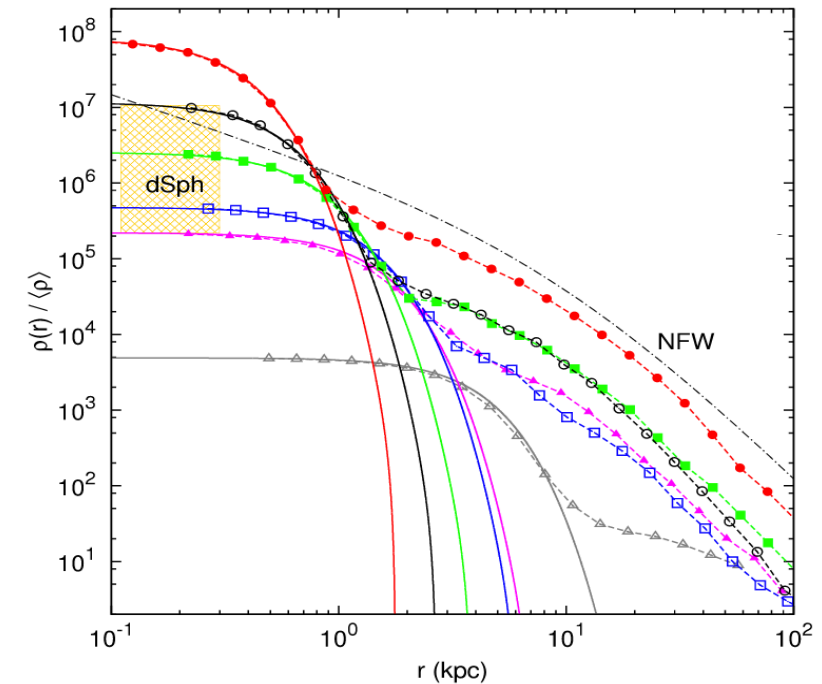
Because of its ultra-light mass \rightarrow Large de Broglie wavelength, $\lambda_{dB} \sim 1/mv$

- $\lambda_{dB} \sim \text{pc} - \text{kpc}$
- Small scales: wavelike behaviour.
- **Solitons:** stable equilibrium configurations \rightarrow **Flat density profile at the center of the halos.**



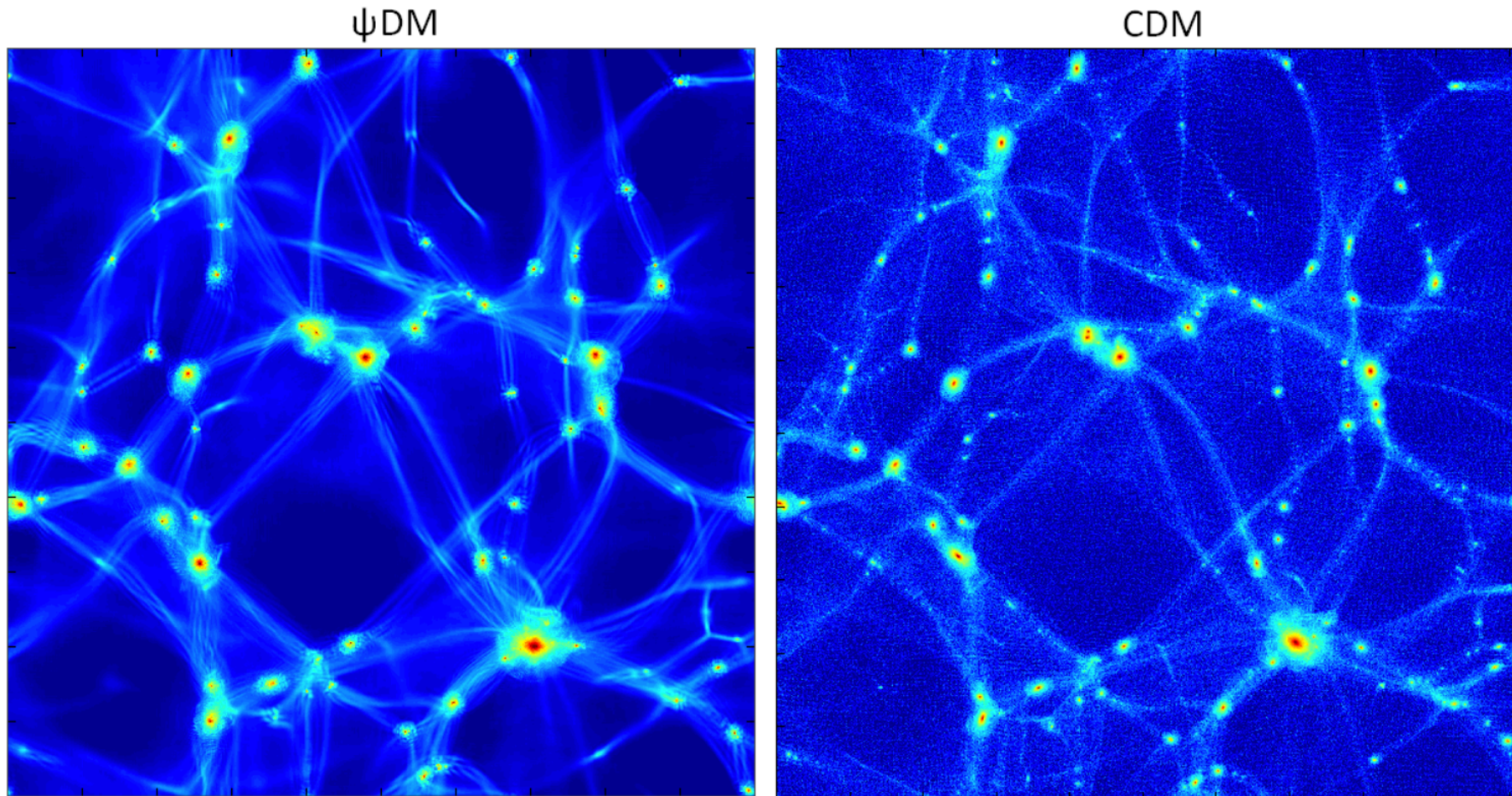
A slice of density field of ψ DM simulation on various scales at $z=0.1$

Schive, Chiueh, and Broadhurst (2014)



Radial density profiles of haloes formed in the ψ DM model

SFDM at large scale scales



SFDM Recover CDM large scale distribution of filaments and voids

Schive, Chiueh, and Broadhurst (2014)

SFDM model

DM is represented by a **scalar field minimally coupled to gravity** given by the Lagrangian:

$$\mathcal{L}_\phi = -\frac{1}{2}g^{\mu\nu}\partial_\mu\phi\partial_\nu\phi - V(\phi),$$

The scalar field potential $V(\phi)$ must have a **parabolic minimum**

$$V(\phi) = \frac{m^2}{2}\phi^2 + V_I(\phi),$$

Fuzzy DM (FDM)

$$V_I(\phi) = 0.$$

m

Quartic model

$$V_I(\phi) = \frac{\lambda_4}{4}\phi^4,$$

m, λ_4

Repulsive $\rightarrow \lambda_4 > 0$

Cosine model

$$V_I(\phi) = M_I^4 \left[\cos(\phi/\Lambda) - 1 + \frac{\phi^2}{2\Lambda^2} \right].$$

m, M_I, Λ

Axion Monodromy

SFDM model

DM is represented by a **scalar field minimally coupled to gravity** given by the Lagrangian:

$$\mathcal{L}_\phi = -\frac{1}{2}g^{\mu\nu}\partial_\mu\phi\partial_\nu\phi - V(\phi),$$

The scalar field potential $V(\phi)$ must have a **parabolic minimum**

$$V(\phi) = \frac{m^2}{2}\phi^2 + V_I(\phi),$$

Fuzzy DM (FDM)

$$V_I(\phi) = 0.$$

m

Quartic model

$$V_I(\phi) = \frac{\lambda_4}{4}\phi^4,$$

m, λ_4

Repulsive $\rightarrow \lambda_4 > 0$

Cosine model

$$V_I(\phi) = M_I^4 \left[\cos(\phi/\Lambda) - 1 + \frac{\phi^2}{2\Lambda^2} \right].$$

m, M_I, Λ

Axion Monodromy

Non-relativistic dynamics for quartic self-interaction

FIELD PICTURE: SCHRÖDINGER—POISSON SYSTEM (SP)

$$i\frac{\partial\psi}{\partial t} = -\frac{1}{2m}\nabla^2\psi + m(\Phi_N + \Phi_I)\psi,$$

$$\nabla^2\Phi_N = 4\pi G_N\rho.$$

Schrödinger equation
(Gross—Pitaevskii)

Poisson equation

Self-interactions (SI):

$$V_I(\phi) = \frac{\lambda_4}{4}\phi^4,$$

strength of the repulsive SI

$$\Phi_I = \frac{3\lambda_4}{4m^3}|\psi|^2.$$

$$\rho = m\psi\psi^*.$$

Self-interaction potential

Ultra-light scalar density

Non-relativistic dynamics of scalar field dark matter

SCHRÖDINGER—POISSON SYSTEM (SP)

$$i\frac{\partial\psi}{\partial t} = -\frac{1}{2m}\nabla^2\psi + m(\Phi_N + \Phi_I)\psi,$$

$$\nabla^2\Phi_N = 4\pi G_N\rho.$$

Schrodinger equation
(Gross—Pitaevskii)

Poisson equation

Self-interactions (SI):

$$V_I(\phi) = \frac{\lambda_4}{4}\phi^4,$$

strength of the repulsive SI

$$\Phi_I = \frac{3\lambda_4}{4m^3}|\psi|^2.$$

Self-interaction potential

$$\rho = m\psi\psi^*.$$

Ultra-light scalar density

HYDRODYNAMICAL PICTURE

Madelung form $\psi \rightarrow \{\rho, S, \vec{v}\},$

$$\psi = \sqrt{\frac{\rho}{m}}e^{iS}, \quad \vec{v} = \frac{\nabla S}{m},$$

$$\begin{aligned} \frac{\partial\rho}{\partial t} + \nabla \cdot (\rho\vec{v}) &= 0, \\ \frac{\partial\vec{v}}{\partial t} + (\vec{v} \cdot \nabla)\vec{v} &= -\nabla(\Phi_N + \Phi_Q + \Phi_I). \end{aligned}$$

$$\nabla^2\Phi_N = 4\pi G_N\rho.$$

Continuity equation

Euler equation

Poisson equation

Quantum pressure

$$\Phi_Q = -\frac{\nabla^2\sqrt{\rho}}{2m^2\sqrt{\rho}}.$$

Non-relativistic dynamics of scalar field dark matter

SCHRÖDINGER—POISSON SYSTEM (SP)

$$i\frac{\partial\psi}{\partial t} = -\frac{1}{2m}\nabla^2\psi + m(\Phi_N + \Phi_I)\psi,$$

$$\nabla^2\Phi_N = 4\pi G_N\rho.$$

Schrodinger equation
(Gross—Pitaevskii)

Poisson equation

Self-interactions (SI):

$$V_I(\phi) = \frac{\lambda_4}{4}\phi^4,$$

strength of the repulsive SI

$$\Phi_I = \frac{3\lambda_4}{4m^3}|\psi|^2.$$

$$\rho = m\psi\psi^*.$$

Self-interaction potential

Ultra-light scalar density

HYDRODYNAMICAL PICTURE

Madelung form $\psi \rightarrow \{\rho, S, \vec{v}\},$

$$\psi = \sqrt{\frac{\rho}{m}}e^{iS}, \quad \vec{v} = \frac{\nabla S}{m},$$

$$\begin{aligned} \frac{\partial\rho}{\partial t} + \nabla \cdot (\rho\vec{v}) &= 0, \\ \frac{\partial\vec{v}}{\partial t} + (\vec{v} \cdot \nabla)\vec{v} &= -\nabla(\Phi_N + \Phi_Q + \Phi_I), \\ \nabla^2\Phi_N &= 4\pi G_N\rho. \end{aligned}$$

Continuity equation

Euler equation

Poisson equation

Quantum pressure

$$\Phi_Q = -\frac{\nabla^2\sqrt{\rho}}{2m^2\sqrt{\rho}}.$$

$$\Phi_N + \Phi_I + \Phi_Q = \alpha,$$

Soliton: hydrostatic equilibrium

Self-interacting soliton

Soliton: Hydrostatic equilibrium

$$\Phi_N + \Phi_I + \Phi_Q = \alpha,$$

Thomas-Fermi regime $\rightarrow \Phi_Q \ll \Phi_I$

Soliton TF limit

$$\Phi_N + \Phi_I = \alpha,$$

Helmholtz equation:

$$\nabla^2 \rho = -\frac{16\pi G m^4}{3\lambda_4} \rho. \quad \rightarrow \quad \rho''(r) + \frac{2}{r} \rho'(r) + \frac{1}{r_a^2} \rho(r) = 0.$$

In this approximation, the soliton density profile :

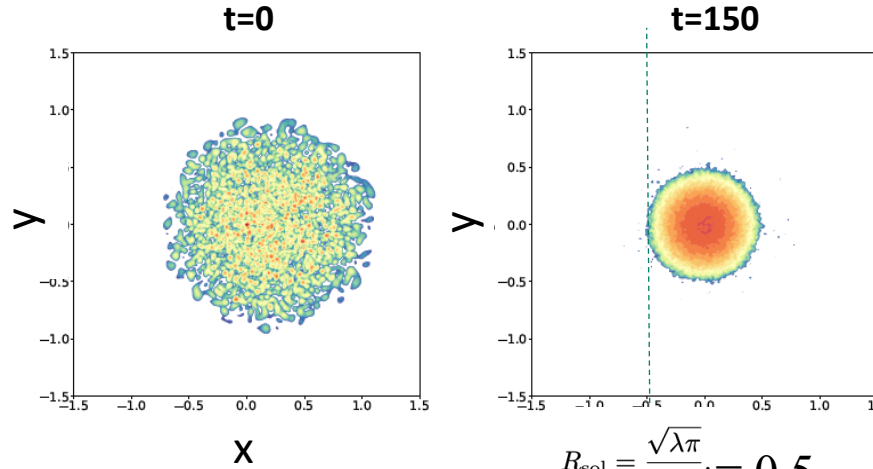
$$\rho_{\text{sol}}(r) = \rho_{0\text{sol}} \frac{\sin(\pi r/R_{\text{sol}})}{\pi r/R_{\text{sol}}},$$

$$R_{\text{sol}} = \pi r_a, \quad \text{with } r_a^2 = \frac{3\lambda_4}{16\pi G_N m^4} :$$

r_a sets Jeans length !

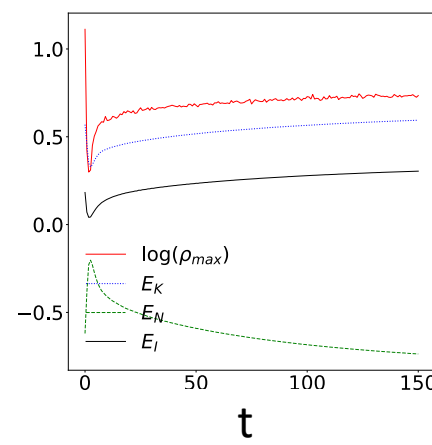
I) Flat halo with r_a of the order of the system

Large soliton, $R_{\text{sol}} = 0.5$: interactions r_a of the order of the system

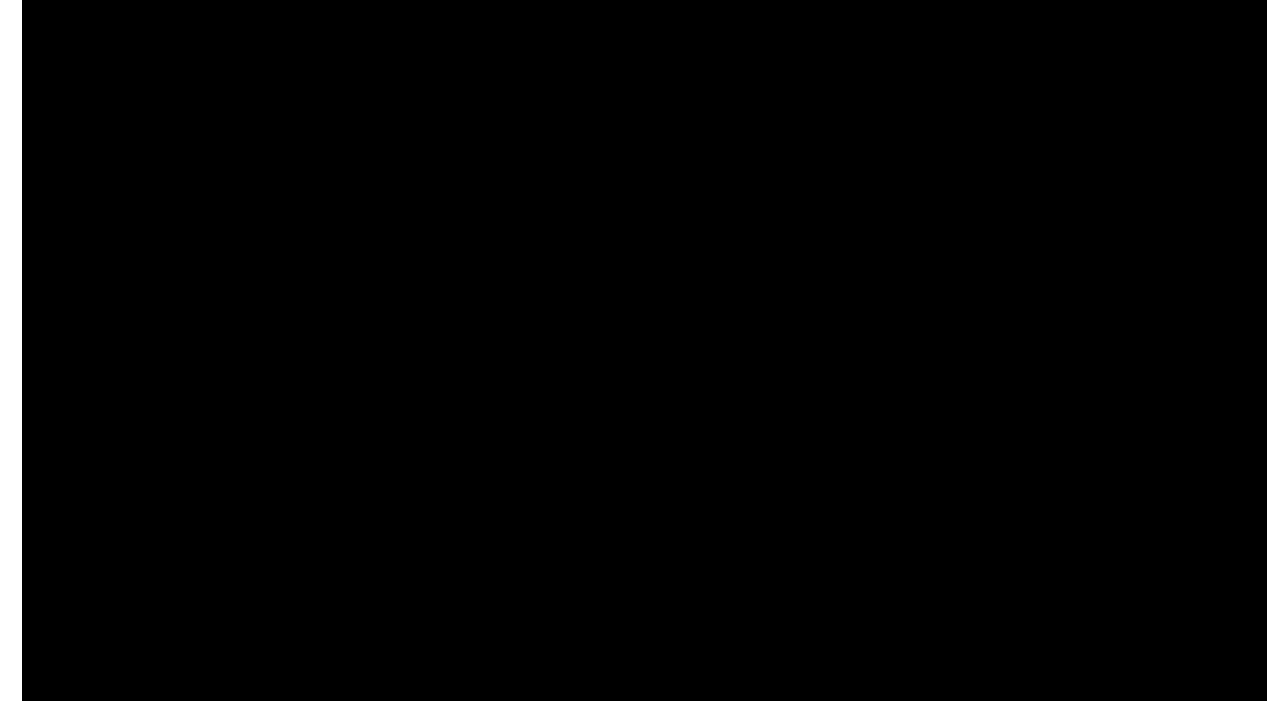
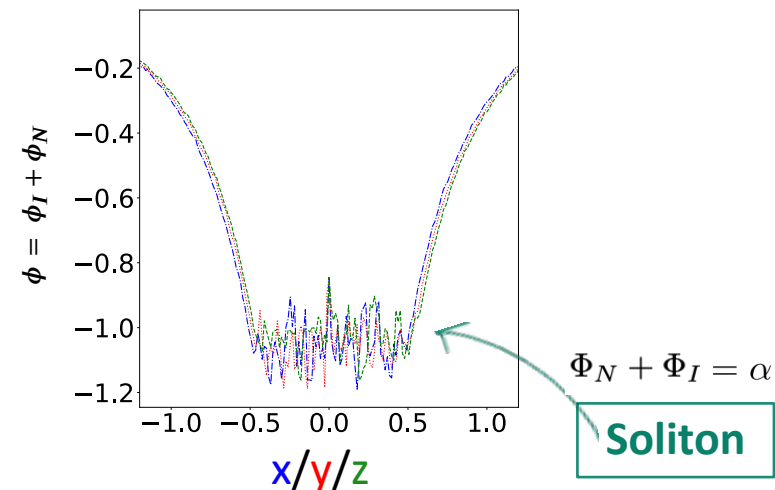


$$R_{\text{sol}} = \frac{\sqrt{\lambda\pi}}{2} = 0.5$$

ρ_{\max} , E_K , E_I , E_N



Potential at $t=150$



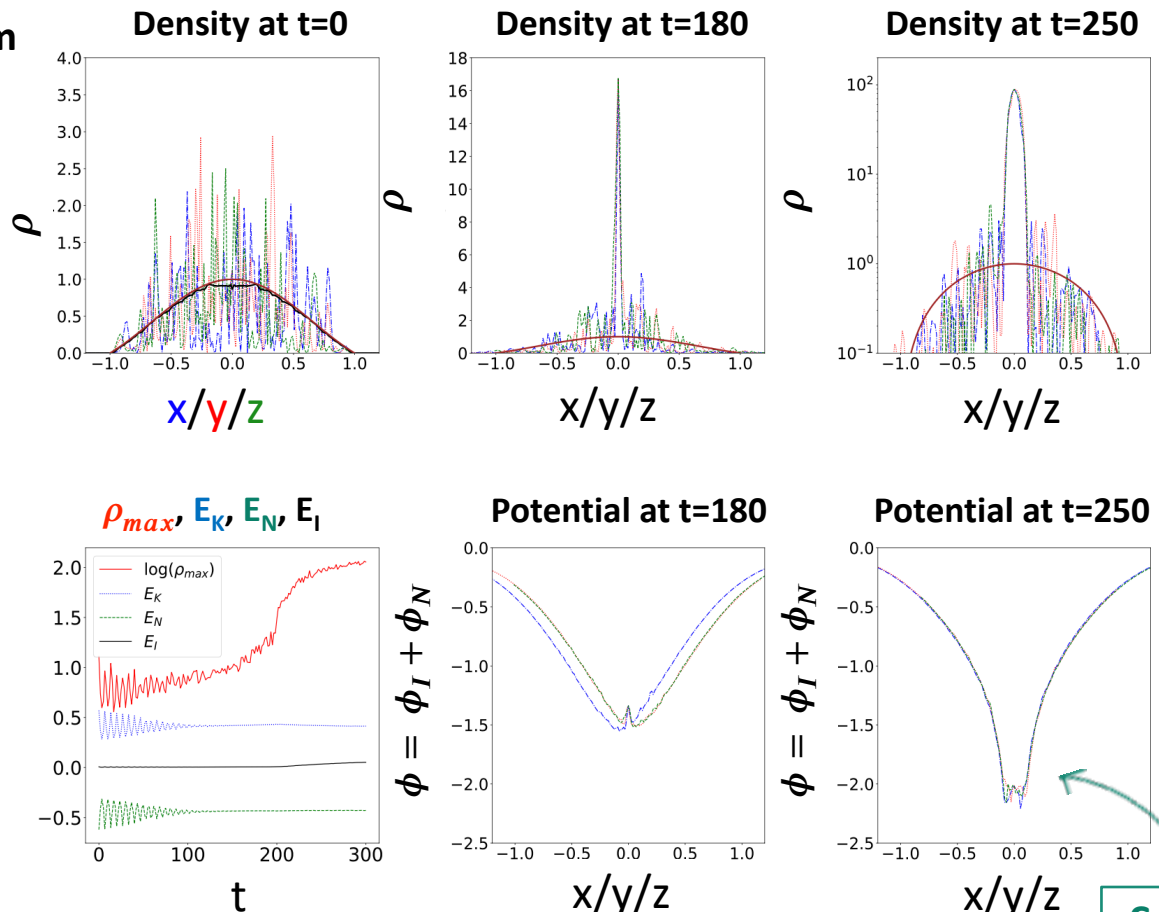
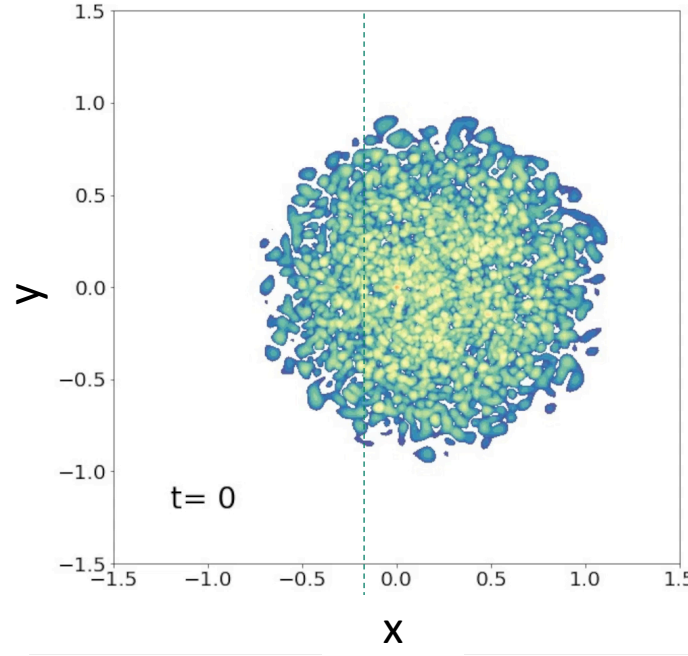
Flat halo with r_a of the order of the system

R.Galazo-García et al. (2024) acknowledgements to Jean Charles Lambert

II) Flat halo with r_a much smaller than system

Small soliton, $R_{\text{sol}} = 0.1$: interactions r_a much smaller than the system

Density slice 2D (x, y) at $z=r_{\text{max}}, (\rho_{\text{max}})$



- By $t \sim 100$, the halo relaxes to a quasi-stationary state.
- At $t \sim 180$, FDM peak.
- At $t \sim 200$, self-interacting soliton forms, $R_{\text{sol}} = 0.1$.

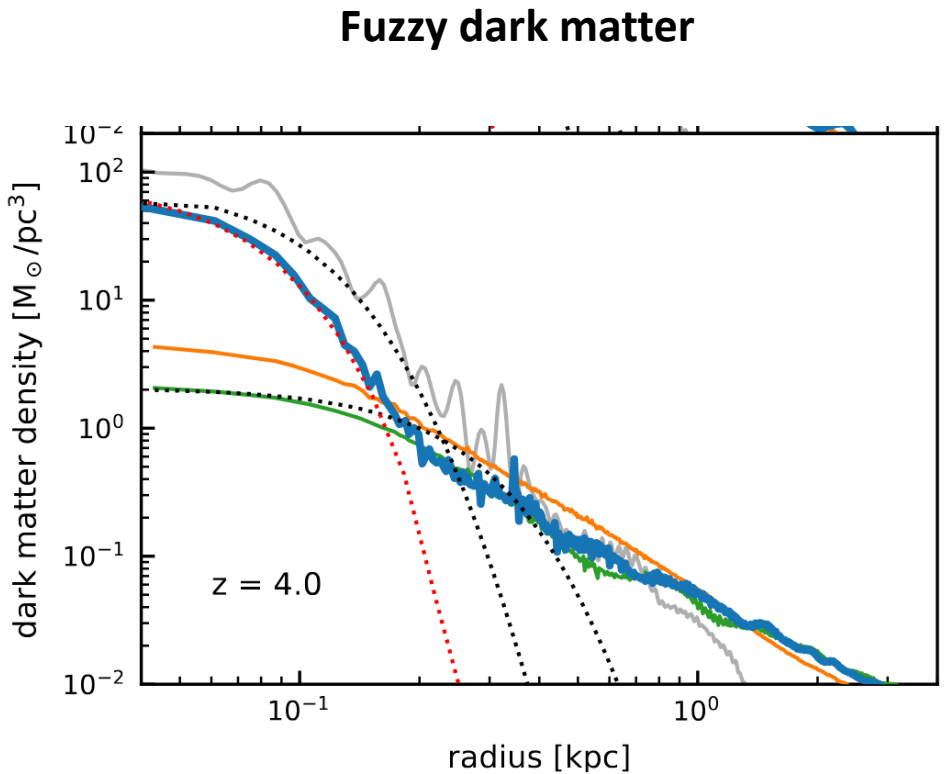
R.Galazo-García, P.Brax and P.Valageas (2024)

Transition from a **FDM phase** to a **self-interacting phase**.

Impact of baryons on self-interacting soliton cores ?

- Compression of the soliton density profile

- Analytical solution for the inhomogeneous equation in the quartic self-interacting scenario



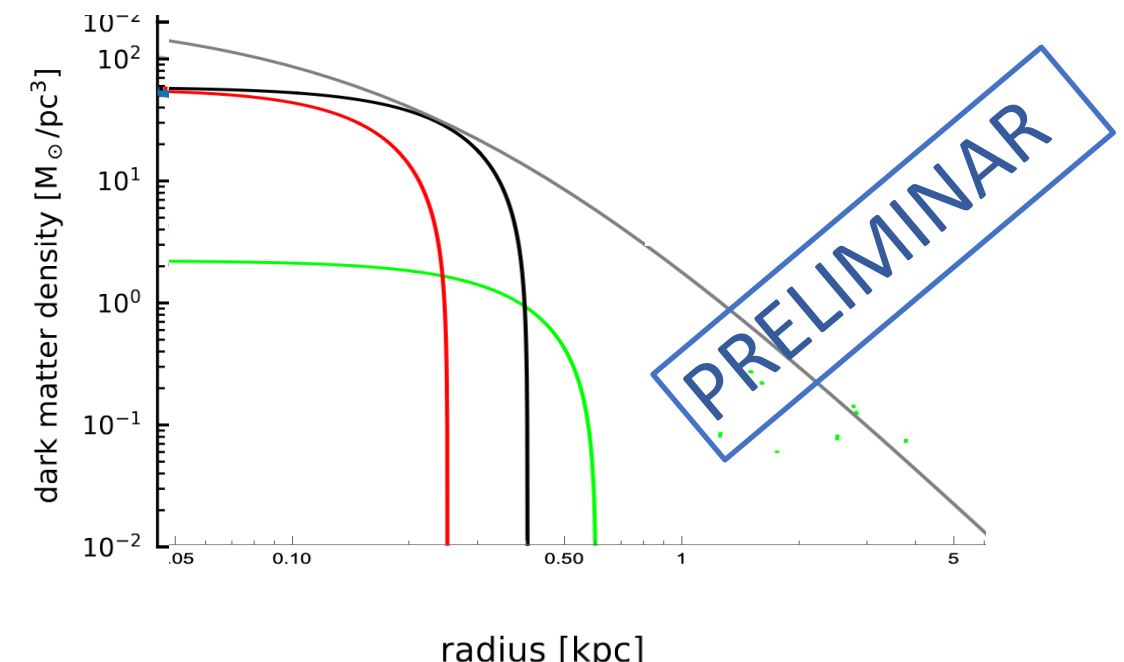
Jan Veltmaat, Bodo Schwabe, and Jens C. Niemeyer (2020)

Self-interacting scalar field dark matter

$$\rho_b(r) = \frac{\rho_{b0}}{(1 + r/r_{b0})^3},$$

↓

$$\rho''(r) + \frac{2}{r}\rho'(r) + \frac{1}{r_a^2}\rho(r) + \rho_b(r) = 0.$$

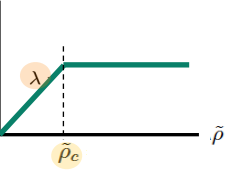


Non-polynomial self-interacting

$$i\epsilon \frac{\partial \tilde{\psi}}{\partial t} = -\frac{\epsilon^2}{2} \tilde{\nabla}^2 \tilde{\psi} + (\tilde{\Phi}_N + \tilde{\Phi}_I) \tilde{\psi},$$

$$\tilde{\nabla}^2 \tilde{\Phi}_N = 4\pi \tilde{\rho}, \quad \text{with} \quad \tilde{\rho} = |\tilde{\psi}|^2,$$

$$\tilde{\Phi}_I(\tilde{\rho}) = \begin{cases} \lambda \tilde{\rho} & \text{if } \tilde{\rho} < \tilde{\rho}_c \\ \lambda \tilde{\rho}_c & \text{if } \tilde{\rho} > \tilde{\rho}_c \end{cases}$$



Low density regime:

$$\text{TF regime : } \Phi_N + \Phi_I = \mu.$$

High density regime:

$$\text{FDM regime : } \Phi_Q + \Phi_N = \mu - \lambda \rho_c,$$

Transition from a self-interacting phase to a FDM phase !

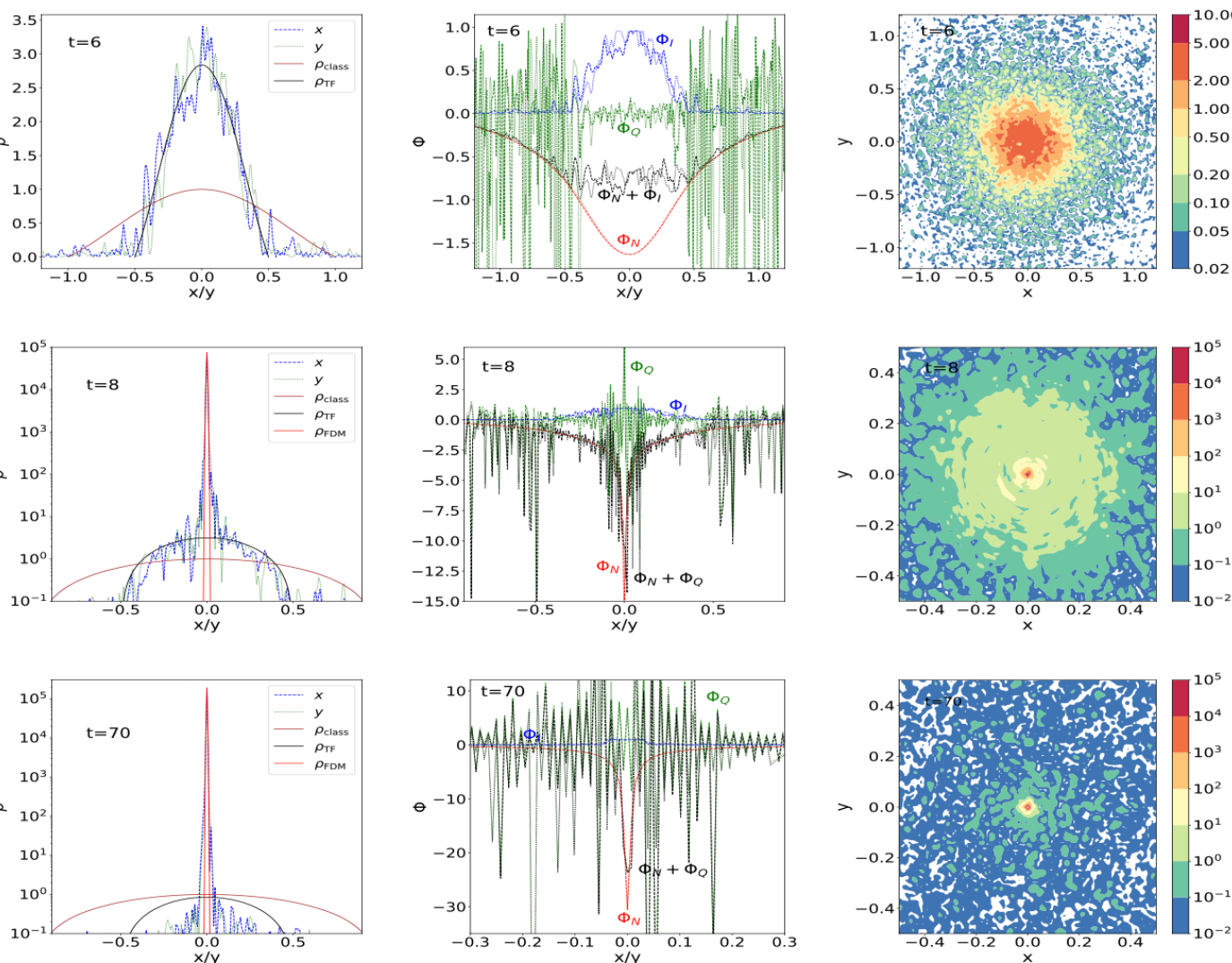


FIG. 4. Evolution of a halo with $R_{\text{TF}} = 0.5$ and $\rho_c = 3$.

Upcoming preprint, check the arXiv these weeks!! R.Galazo-García, P.Brax and P.Valageas

Gaussian ansatz to describe the transition

$$\rho(r) = \rho_0 e^{-(r/R)^2}, \quad \psi = \sqrt{\rho}, \quad \text{with} \quad \rho_0 = \frac{M}{\pi^{3/2} R^3}.$$

$$E_{\text{tot}} = E_K + E_N + E_I = \int d\vec{x} \left(\frac{\epsilon^2}{2} |\nabla \psi|^2 + \frac{1}{2} \rho \Phi_N + \mathcal{V}_I \right)$$

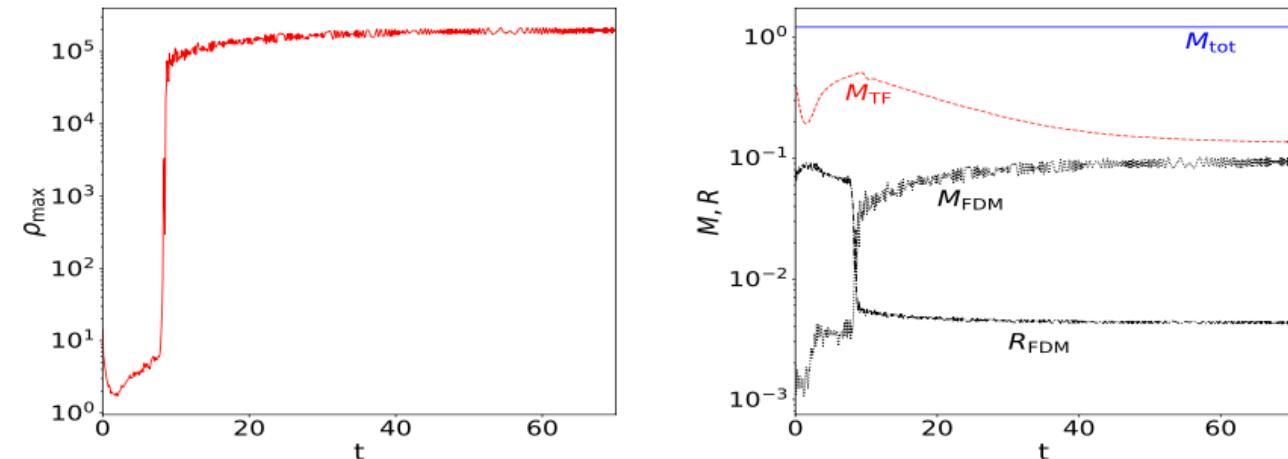
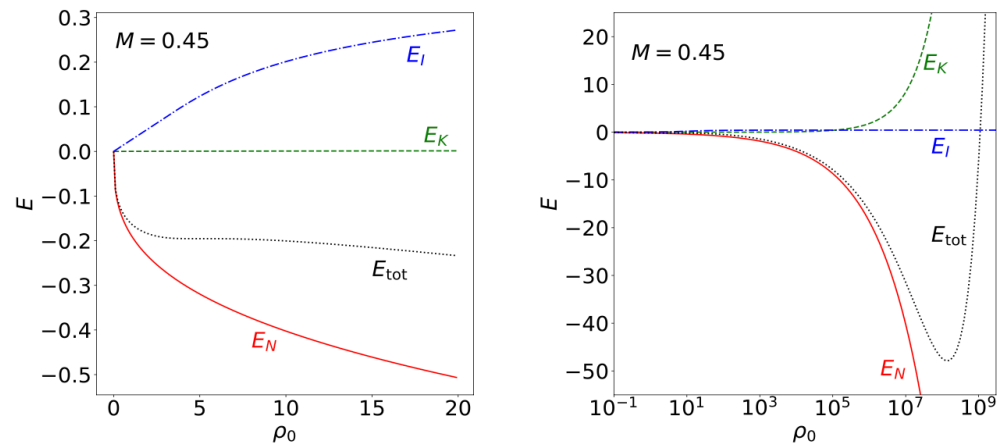
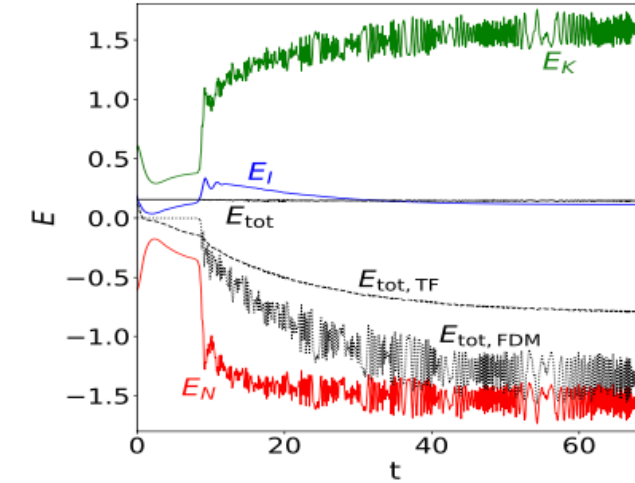
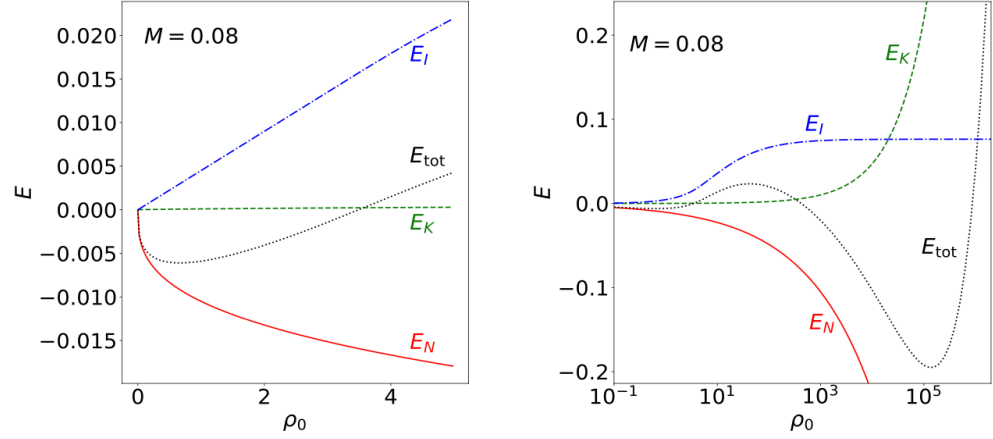


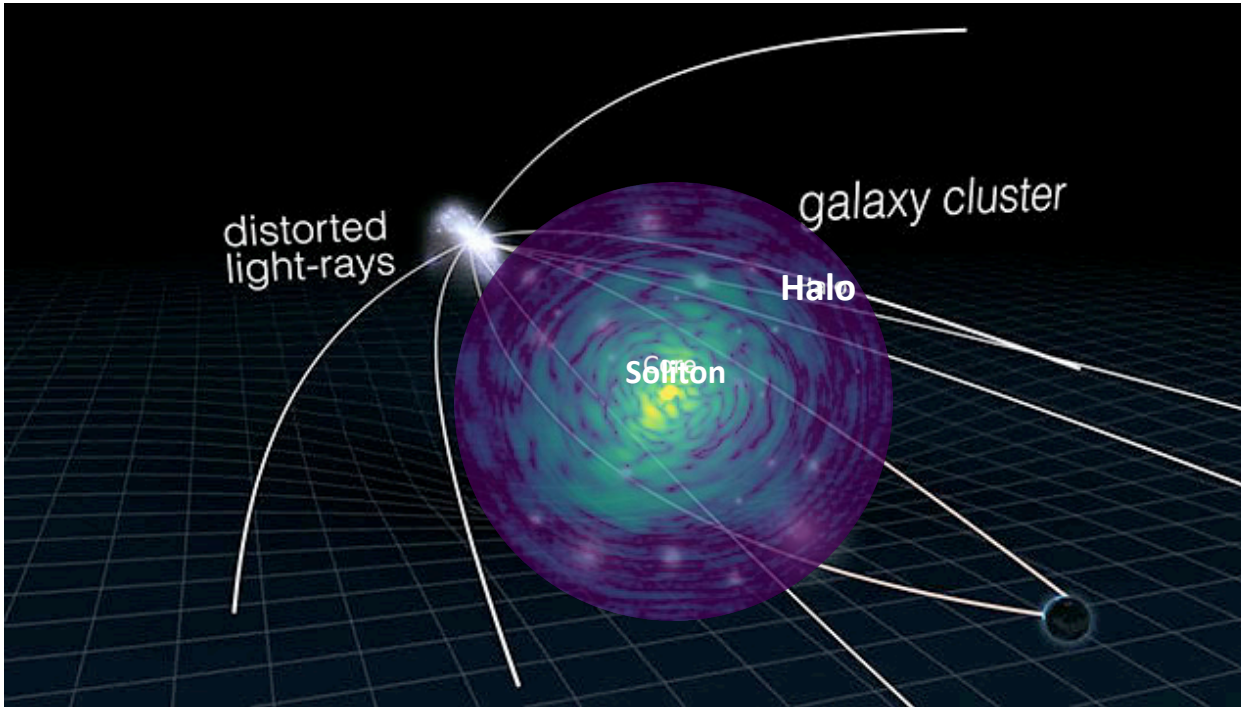
FIG. 7. [$R_{\text{TF}} = 0.5$, $\rho_c = 3$.] Energy of a Gaussian density profile.

Strong gravitational lensing signatures in galaxy clusters for self-interacting SFDM

- DM structures (solitons) leave a gravitational imprint on the multiple images of lensed sources.
- Multiple images provide a key test of different DM models Independent of the baryonic content.

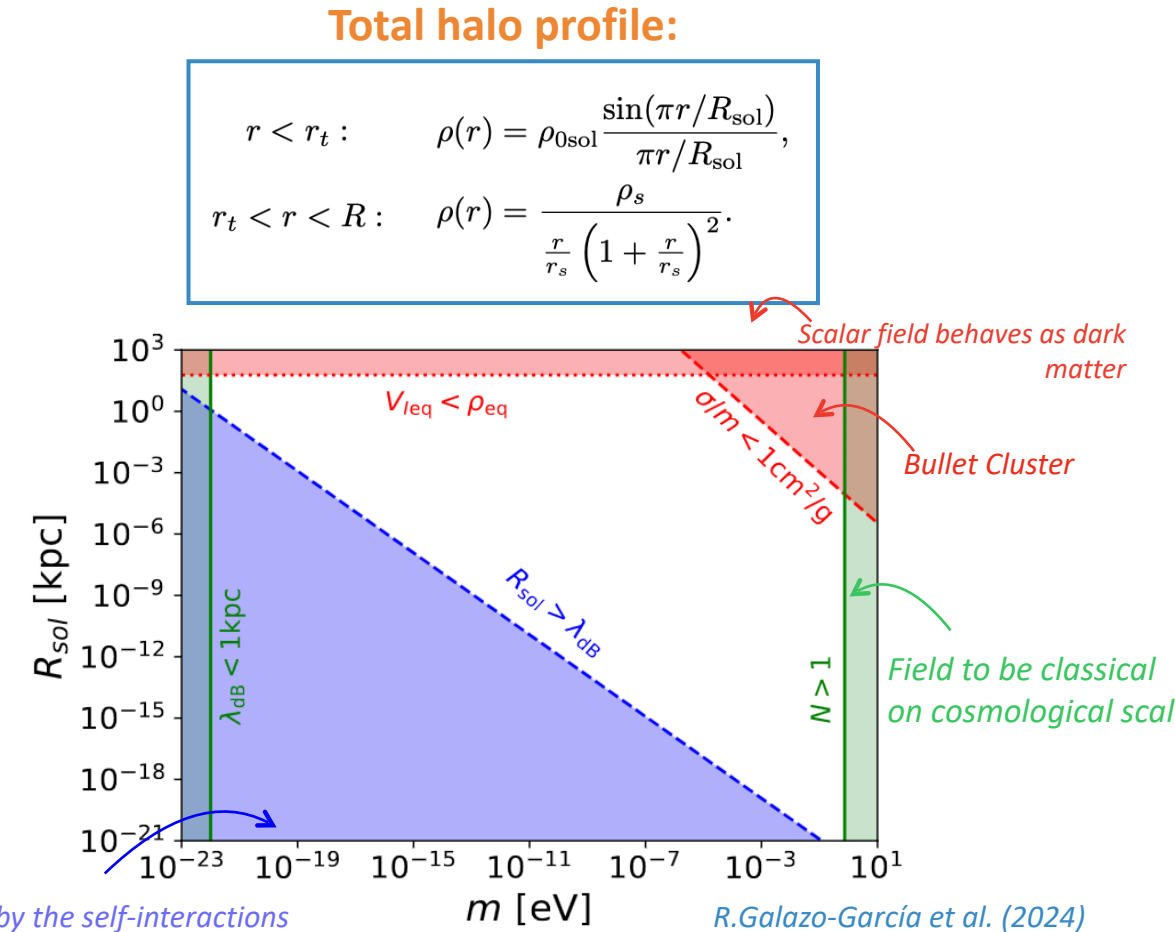
Self Interaction potential :

$$\Phi_I = \frac{3\lambda_4}{4m^3} |\psi|^2.$$



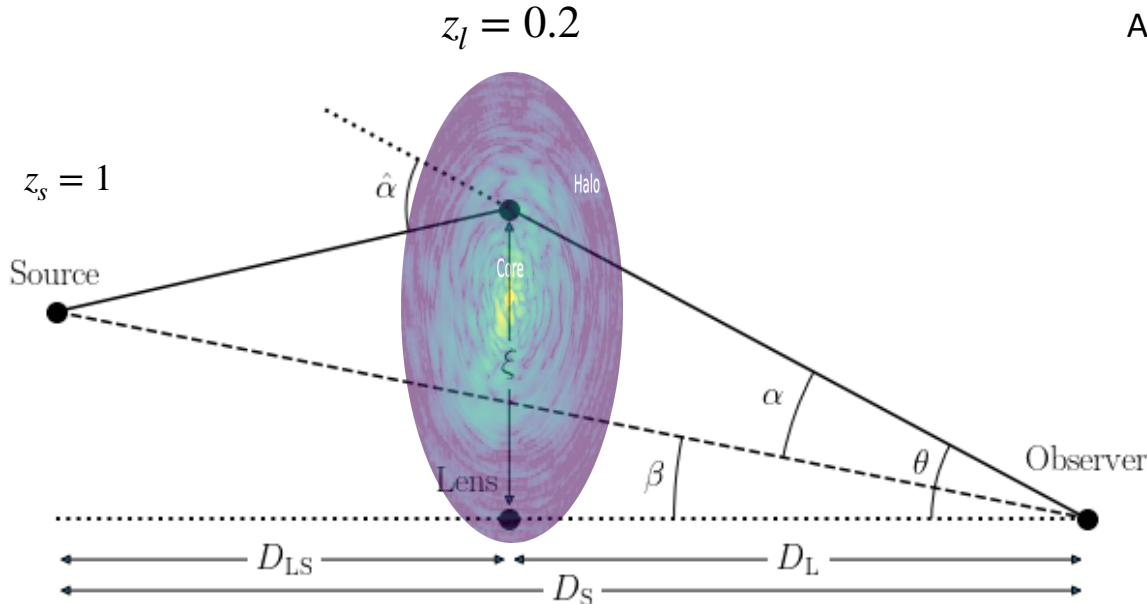
Scheme of strong gravitational lensing with SFDM
Credit 1: NASA, ESA & L. Calçada & Credit 2:

Soliton is governed by the self-interactions



General lensing equations

- We assume spherical symmetry and the thin approximation size of the object is negligible compare to the angular distances.



Actual unobservable angular position to the source

$$\beta = \theta - \frac{D_{LS}}{D_S} \hat{\alpha}(\xi)$$

Observable apparent angular position to the image

$$\Sigma_{\text{cr}} \equiv \frac{c^2}{4\pi G} \frac{D_s}{D_1 D_{ls}}$$

Deflection angle

$$\hat{\alpha}(\vec{\xi}) = \frac{4G}{c^2} \int \frac{(\vec{\xi} - \vec{\xi}') \Sigma(\vec{\xi}')}{|\vec{\xi} - \vec{\xi}'|} d^2 \xi'$$

Surface mass density

$$\Sigma(\vec{\xi}) = \int \rho(\vec{\xi}, z) dz$$

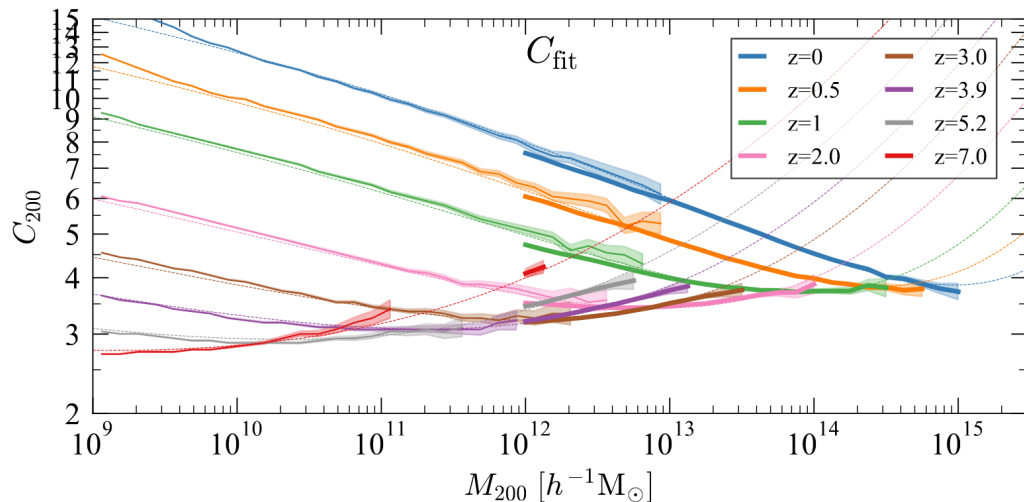
Excess surface mass density

$$\Delta\Sigma(R) \equiv \bar{\Sigma}(R) - \Sigma(R) = \Sigma_{\text{cr}} \gamma_+(R)$$

NFW - Deflection angle and surface mass density

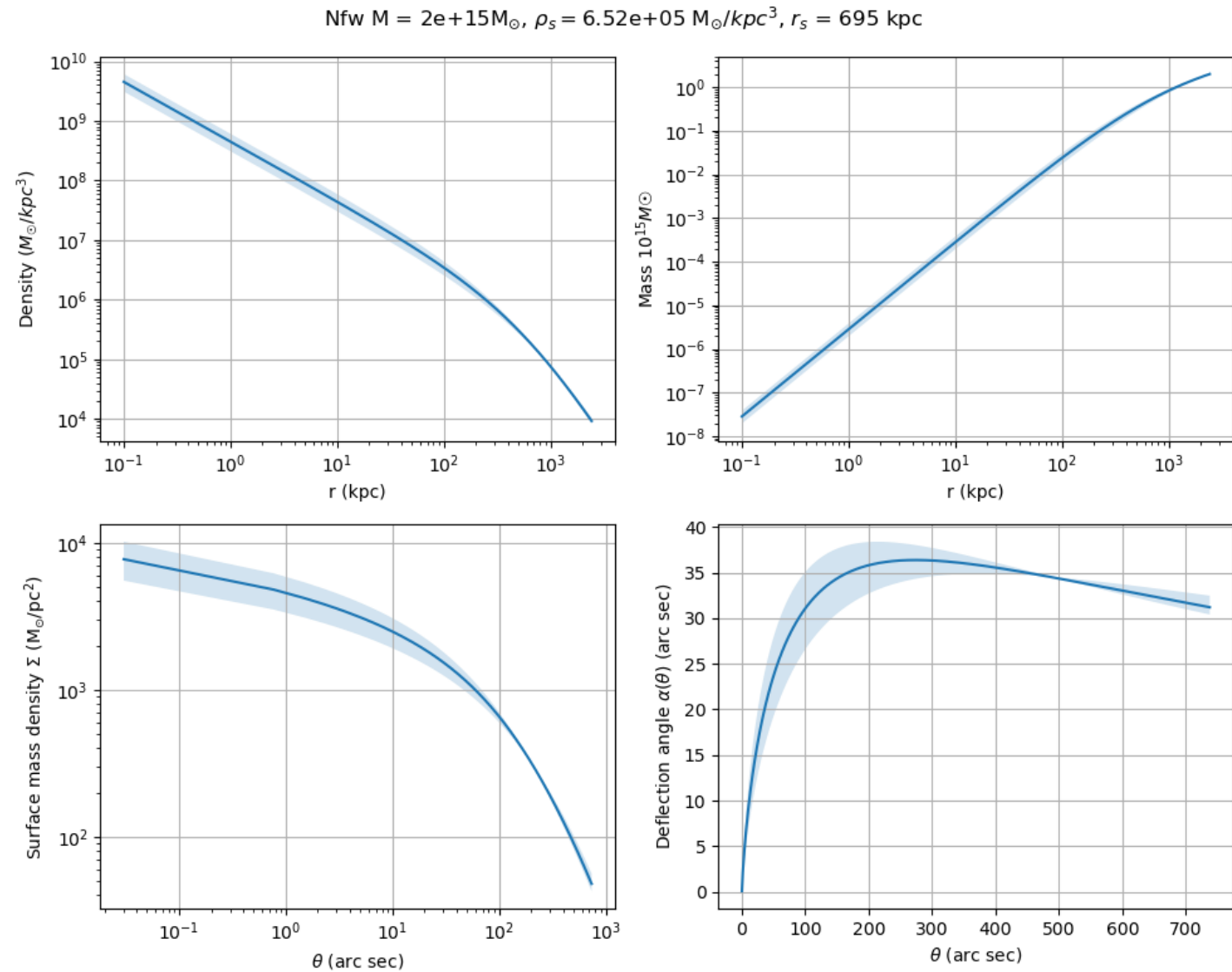


- We build the NFW from the total mass of the system (r_{200}) and the concentration (r_s), and we get ρ_s .



Mass-concentration relation of halos for the Uchuu simulation

Ishiyama et al. (2021)



Total profile

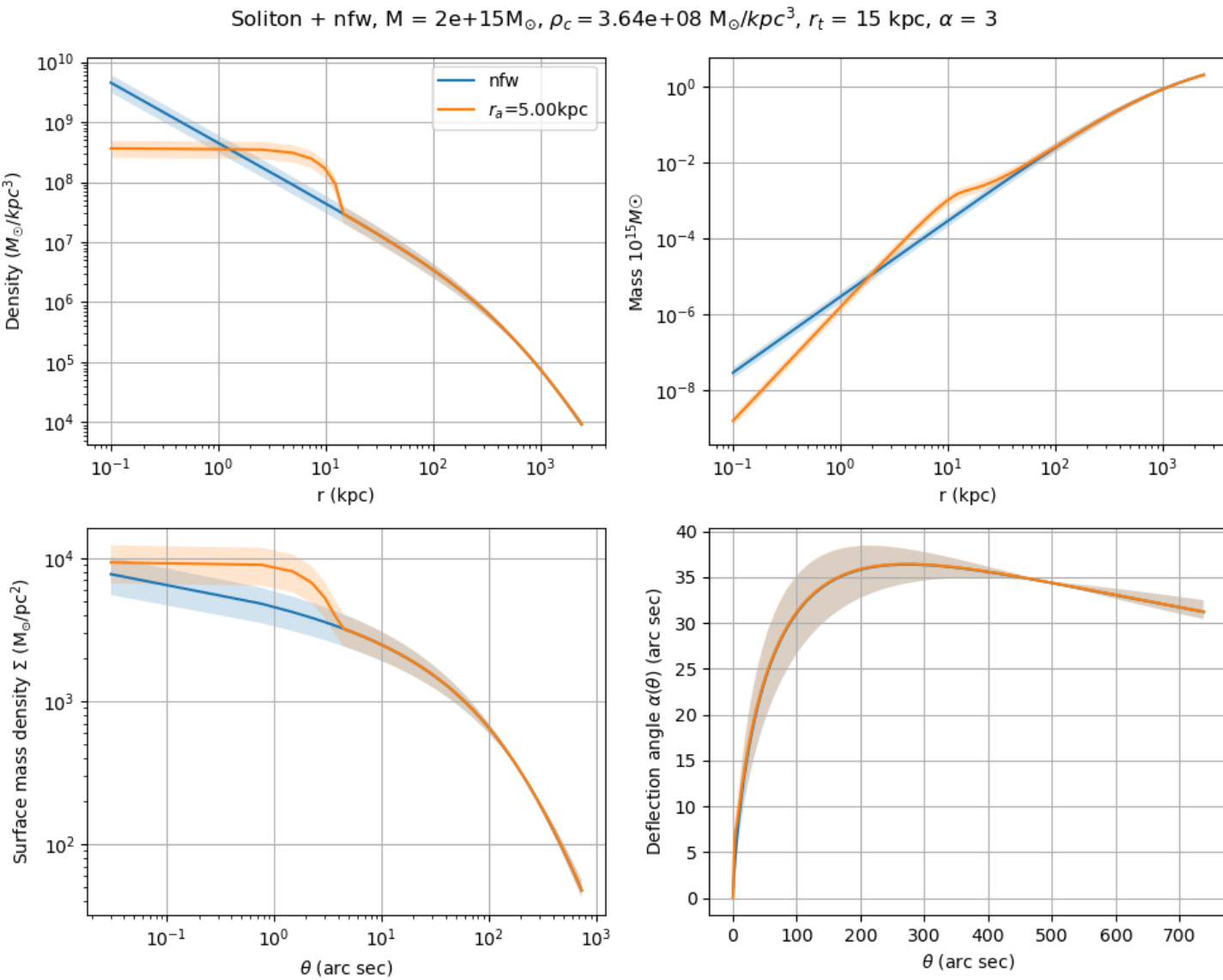


- We choose the model to study $R_{sol} = \pi r_a$

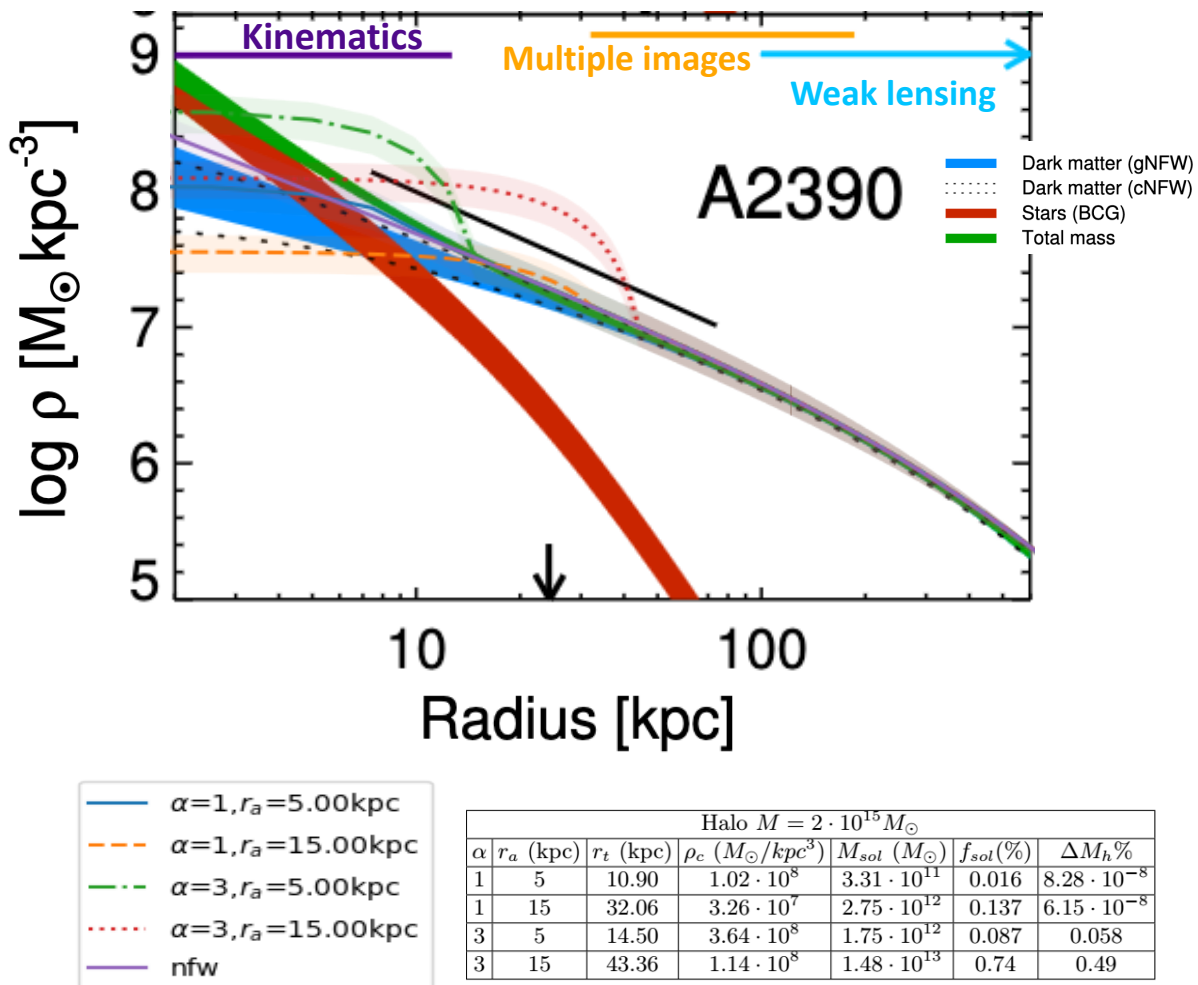
$$r < r_t : \quad \rho(r) = \rho_{0sol} \frac{\sin(\pi r/R_{sol})}{\pi r/R_{sol}},$$

$$r_t < r < R : \quad \rho(r) = \frac{\rho_s}{\frac{r}{r_s} \left(1 + \frac{r}{r_s}\right)^2}.$$

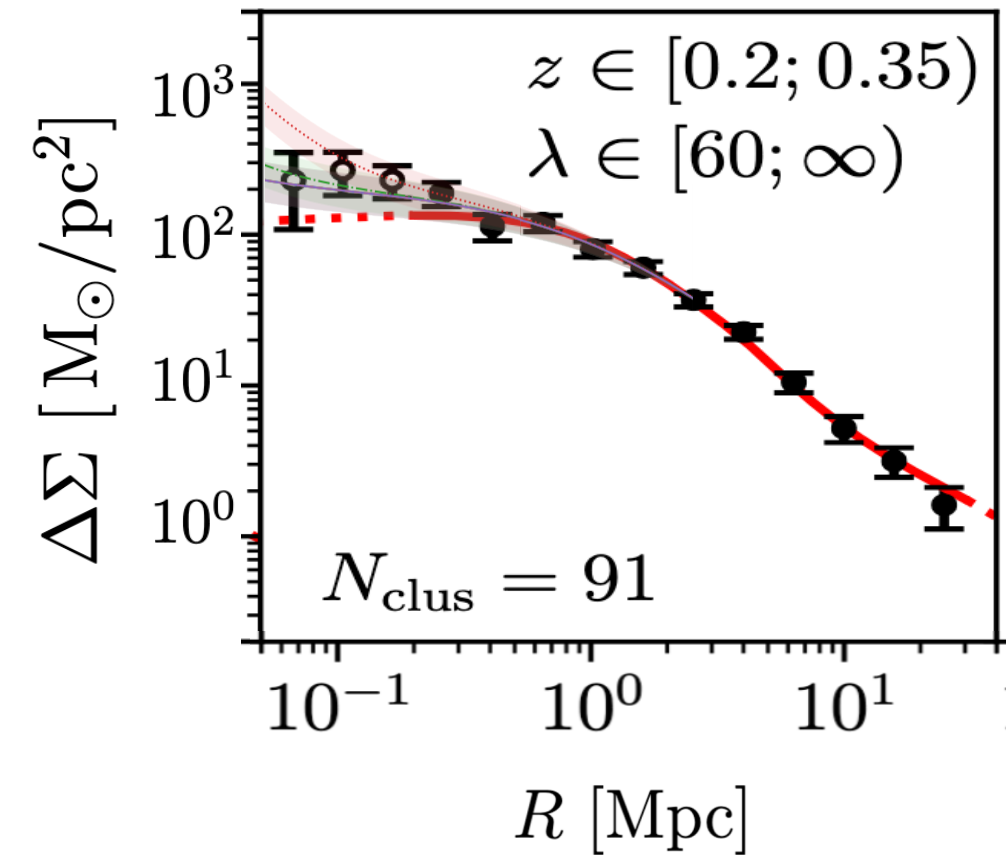
- We calculate the value of r_t and ρ_{0sol} such that $M_{sol}(< r_t) = \alpha M_{NFW}(< r_t)$ and the total mass of the system is conserved.
- We have slight flexibility in the choice of α as long as we are in the Newtonian regime ($M \sim 10^{17} M_\odot$) and the mass of the system varies minimally.



Study case: Halo $M \sim 10^{15} M_\odot$

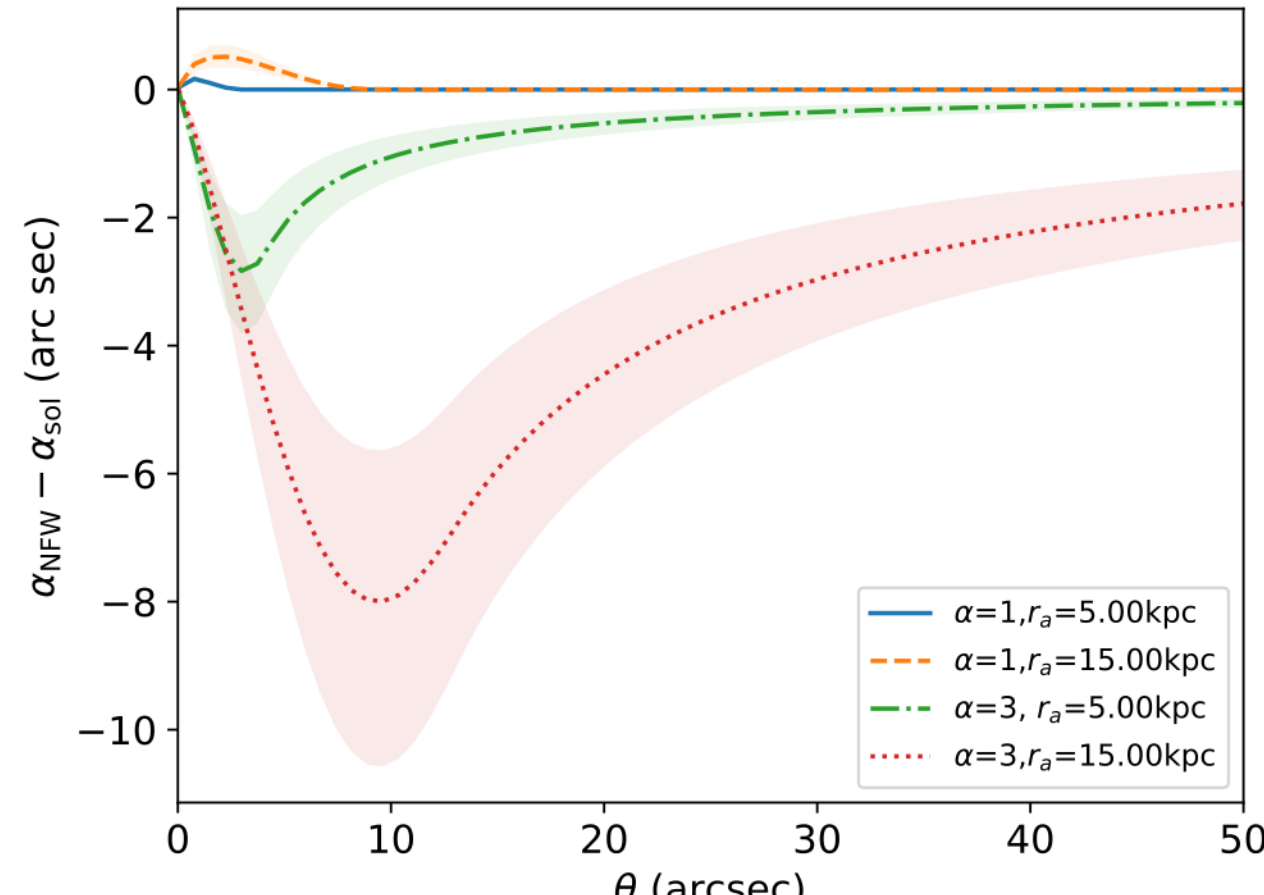


Comparison with Andrew B. Newman, Tommaso Treu, Richard S. Ellis, and David J. Sand, 2013

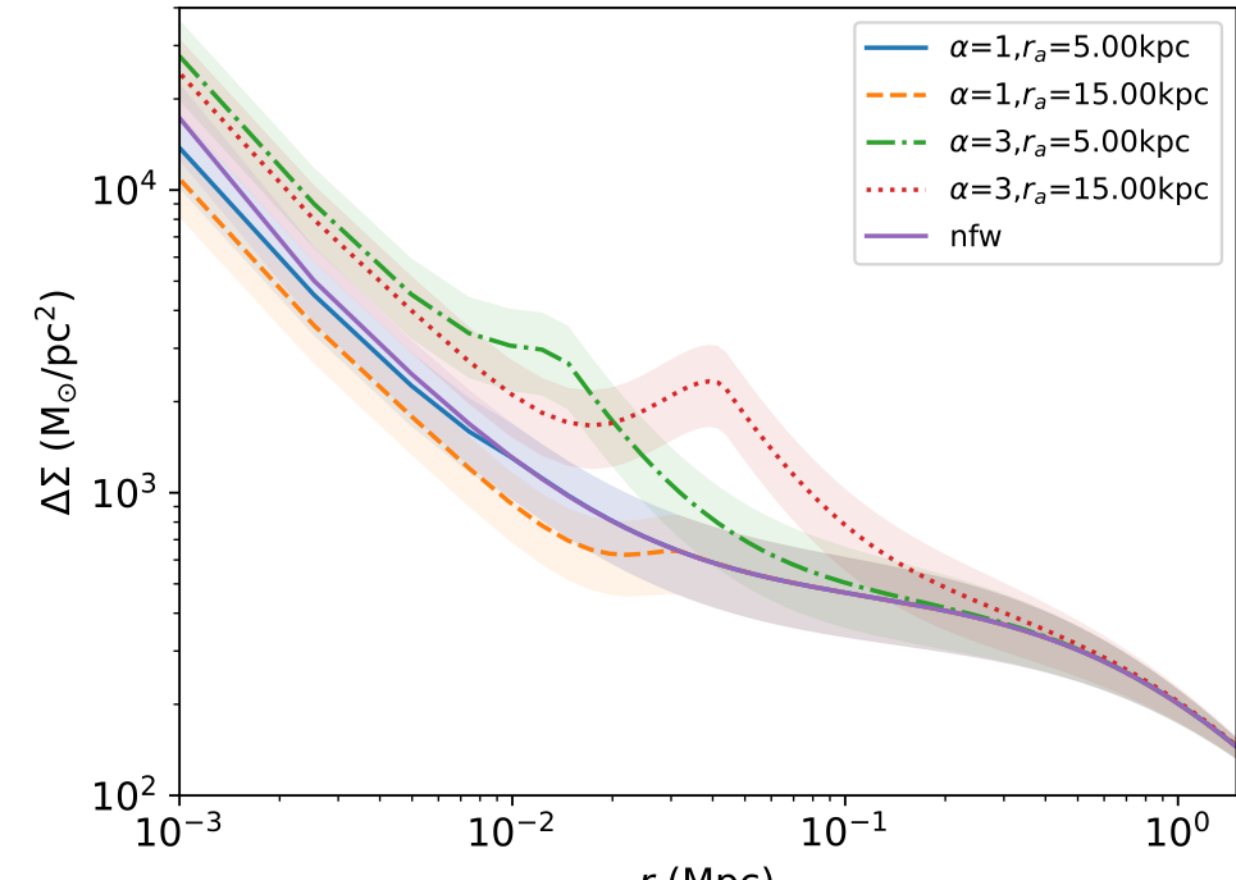


Comparison with Dark Energy Survey Year 1 Results: Weak Lensing Mass Calibration of redMaPPer Galaxy Clusters 2018

Study case: Halo $M \sim 10^{15} M_\odot$



Difference of deflection angle NFW-Soliton



Excess surface mass density

Outlook

- **SFDM as a Strong Alternative:** SFDM presents a promising alternative for describing dark matter.
- **Unique Lensing Patterns:** Differences in SI-SFDM density create distinct gravitational lensing signatures
- **Parameter Constraints:** Preliminary results suggest we can constrain SI-SFDM parameters.
- **Challenges with Massive Clusters:** While the relevant parameter space is more accessible in massive clusters, these clusters pose greater modeling challenges.
- **Insights from Less Massive Clusters:** Less massive clusters provide less constraining data but still offer valuable insights.
- **Soliton Mass Constraints:** We can accurately constrain the soliton mass in SI-SFDM → Core halo relation in this model.
- **Strong Lensing Insights:** Strong lensing can help probe SFDM properties, especially in cluster centers
- **Baryonic effects?**
- **Next step: LENSTOOL Implementation:** Calculating profiles using LENSTOOL enhances our SFDM analysis.

Ultralight self-interacting scalar field dark matter

Thank you for your attention

Raquel Galazo-García



Halo $M = 2 \cdot 10^{15} M_\odot$						
α	r_a (kpc)	r_t (kpc)	ρ_c (M_\odot/kpc^3)	M_{sol} (M_\odot)	$f_{sol}(\%)$	$\Delta M_h\%$
1	5	10.90	$1.02 \cdot 10^8$	$3.31 \cdot 10^{11}$	0.016	$8.28 \cdot 10^{-8}$
1	15	32.06	$3.26 \cdot 10^7$	$2.75 \cdot 10^{12}$	0.137	$6.15 \cdot 10^{-8}$
3	5	14.50	$3.64 \cdot 10^8$	$1.75 \cdot 10^{12}$	0.087	0.058
3	15	43.36	$1.14 \cdot 10^8$	$1.48 \cdot 10^{13}$	0.74	0.49

TABLE IX. Soliton profile configurations for $M = 2 \cdot 10^{15} M_\odot$

Halo $M = 2 \cdot 10^{14} M_\odot$						
α	r_a (kpc)	r_t (kpc)	ρ_c (M_\odot/kpc^3)	M_{sol} (M_\odot)	$f_{sol}(\%)$	$\Delta M_h\%$
1	5	11.21	$6.20 \cdot 10^7$	$2.12 \cdot 10^{11}$	0.11	$8.95 \cdot 10^{-8}$
1	15	33.94	$1.8 \cdot 10^7$	$1.74 \cdot 10^{12}$	0.87	$1.87 \cdot 10^{-9}$
3	5	14.50	$2.18 \cdot 10^8$	$1.05 \cdot 10^{12}$	0.52	0.34
3	15	43.36	$6.30 \cdot 10^7$	$8.15 \cdot 10^{12}$	4.08	2.71

TABLE X. Soliton profile configurations for $M = 2 \cdot 10^{14} M_\odot$

Halo $M = 2 \cdot 10^{13} M_\odot$						
α	r_a (kpc)	r_t (kpc)	ρ_c (M_\odot/kpc^3)	M_{sol} (M_\odot)	$f_{sol}(\%)$	$\Delta M_h\%$
1	5	11.50	$3.76 \cdot 10^7$	$1.34 \cdot 10^{11}$	0.64	$8.54 \cdot 10^{-8}$
1	15	35.83	$9.42 \cdot 10^6$	$9.70 \cdot 10^{11}$	4.85	$6.40 \cdot 10^{-8}$
3	5	14.50	$1.28 \cdot 10^8$	$6.18 \cdot 10^{11}$	3.09	2.06
3	15	44.30	$3.10 \cdot 10^7$	$4.06 \cdot 10^{12}$	20.30	13.54

TABLE XI. Soliton profile configurations for $M = 2 \cdot 10^{13} M_\odot$

$M_h(M_\odot)$	Fit $\rho_s(M_\odot/kpc^3)$	Fit r_s (kpc)
$2 \cdot 10^{13}$	$2.90 \cdot 10^5 \pm 0.035$	183.34 ± 2.83
$2 \cdot 10^{14}$	$2.40 \cdot 10^5 \pm 1.03$	429.65 ± 6.46
$2 \cdot 10^{15}$	$3.97 \cdot 10^5 \pm 1.03$	784.85 ± 9.86

TABLE V. NFW with $\alpha = 1$, $\beta = 3$, $\gamma = 1.5$

$$\rho(r) = \frac{\rho_s}{\left(\frac{r}{r_s}\right)^\gamma \left(1 + \left(\frac{r}{r_s}\right)^\alpha\right)^{(\beta-\gamma)/\alpha}}$$

TABLE 8
NFW PARAMETERS DERIVED FROM X-RAY AND LENSING ANALYSES

Cluster	r_s (kpc)	X-Ray	Source	r_s (kpc)	Lensing (Strong + Weak)	$\log M_{200} / M_\odot$	r_{200} (kpc)
		c_{200}			c_{200}		
MS2137	180^{+20}_{-20}	$8.19^{+0.54}_{-0.56}$	S07	119^{+49}_{-32}	$11.03^{+2.81}_{-2.39}$	$14.56^{+0.13}_{-0.11}$	1318^{+140}_{-107}
A963	390^{+120}_{-80}	$4.73^{+0.84}_{-0.77}$	S07	197^{+48}_{-52}	$7.21^{+1.59}_{-0.94}$	$14.61^{+0.11}_{-0.15}$	1430^{+127}_{-151}
A383	470^{+130}_{-100}	$3.8^{+0.7}_{-0.5}$	A08	260^{+59}_{-45}	$6.51^{+0.92}_{-0.81}$	$14.82^{+0.09}_{-0.08}$	1691^{+128}_{-102}
A383 (prolate)	372^{+63}_{-51}	$4.49^{+0.50}_{-0.48}$	14.80 ± 0.08	1665^{+107}_{-95}
A611	320^{+200}_{-100}	$5.39^{+1.60}_{-1.51}$	S07	317^{+57}_{-47}	$5.56^{+0.65}_{-0.60}$	14.92 ± 0.07	1760^{+97}_{-89}
A2537	370^{+310}_{-150}	$4.86^{+2.06}_{-1.62}$	S07	442^{+46}_{-44}	$4.63^{+0.35}_{-0.30}$	15.12 ± 0.04	2050^{+65}_{-69}
A2667	700^{+479}_{-207}	$3.02^{+0.74}_{-0.85}$	A03	725^{+118}_{-109}	$2.99^{+0.32}_{-0.27}$	15.16 ± 0.08	2164^{+137}_{-129}
A2390	757^{+1593}_{-393}	$3.20^{+1.59}_{-1.57}$	A03	763^{+119}_{-107}	$3.24^{+0.35}_{-0.31}$	$15.34^{+0.06}_{-0.07}$	2470^{+112}_{-123}

NOTE. — All X-ray fits are to the total gravitating mass and have been standardized to the same cosmology. Sources: S07 = Schmidt & Allen (2007), A08 = Allen et al. (2008), A03 = Allen et al. (2003). The A383 (prolate) row shows a fit to lensing and X-ray data using triaxial isodensity surfaces (Equation 14, and see N11); we report sphericalized NFW parameters in this case.

Non-relativistic dynamics of scalar field dark matter

- At small-scales, expansion of the universe is negligible

$$\phi = \frac{1}{\sqrt{2m}}(\psi e^{-imt} + \psi^* e^{imt}),$$

FIELD PICTURE: SCHRÖDINGER—POISSON SYSTEM (SP)

$$i\frac{\partial\psi}{\partial t} = -\frac{1}{2m}\nabla^2\psi + m(\Phi_N + \Phi_I)\psi,$$

$$\nabla^2\Phi_N = 4\pi G_N\rho.$$

Schrödinger equation
(Gross—Pitaevskii)

Poisson equation

$$\Phi_I(\rho) = \frac{dV_I}{d\rho},$$

$$\rho = m\psi\psi^*.$$

Self-interaction potential

Ultra-light scalar density

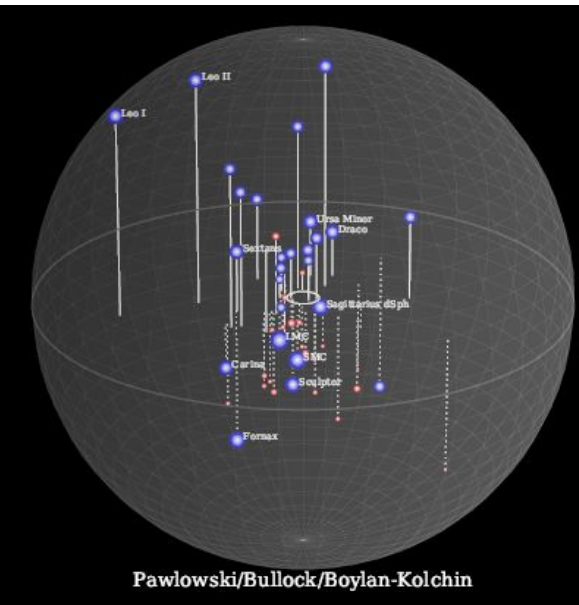
SP system scaling law for FDM or Quartic model

$$\{t \rightarrow \alpha^{-2}t, \vec{x} \rightarrow \alpha^{-1}\vec{x}, \Phi_N \rightarrow \alpha^2\Phi_N, \rho \rightarrow \alpha^4\rho, \psi \rightarrow \alpha^2\psi, \Phi_I \rightarrow \alpha^2\Phi_I, \lambda_4 \rightarrow \alpha^2\lambda_4, E_I \rightarrow \alpha^3E_I, E \rightarrow \alpha^3E\}.$$

SFDM Motivation: Explanation to CDM small-scales tensions

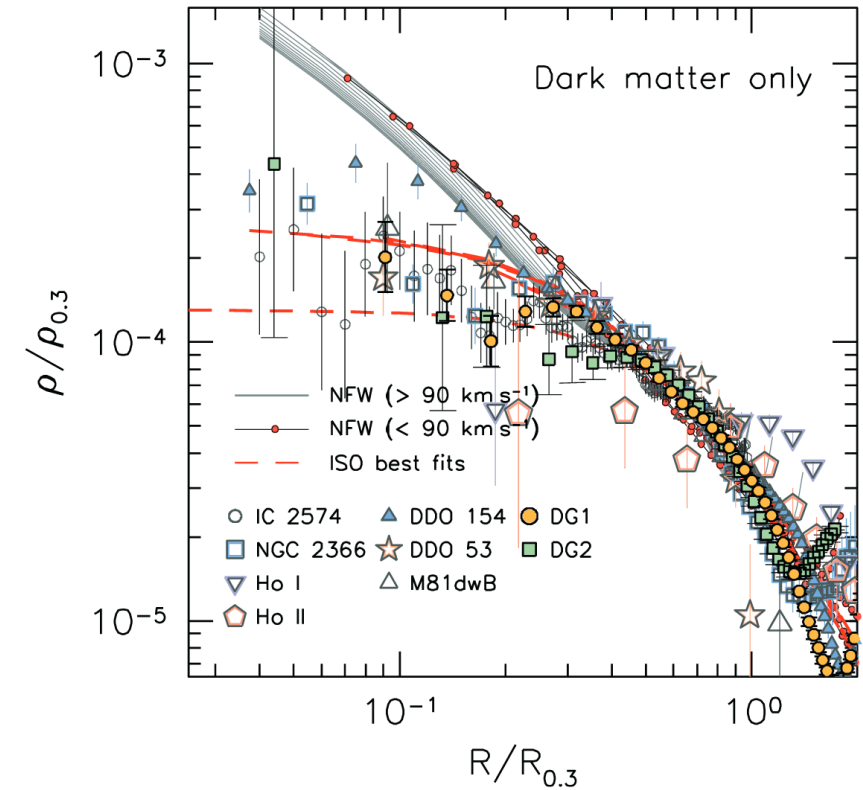


Missing satellite problem



Simulation by V. Robles and T. Kelley
and collaborators.

James S. Bullock, M. Boylan-Kolchin,
M. Pawlowski



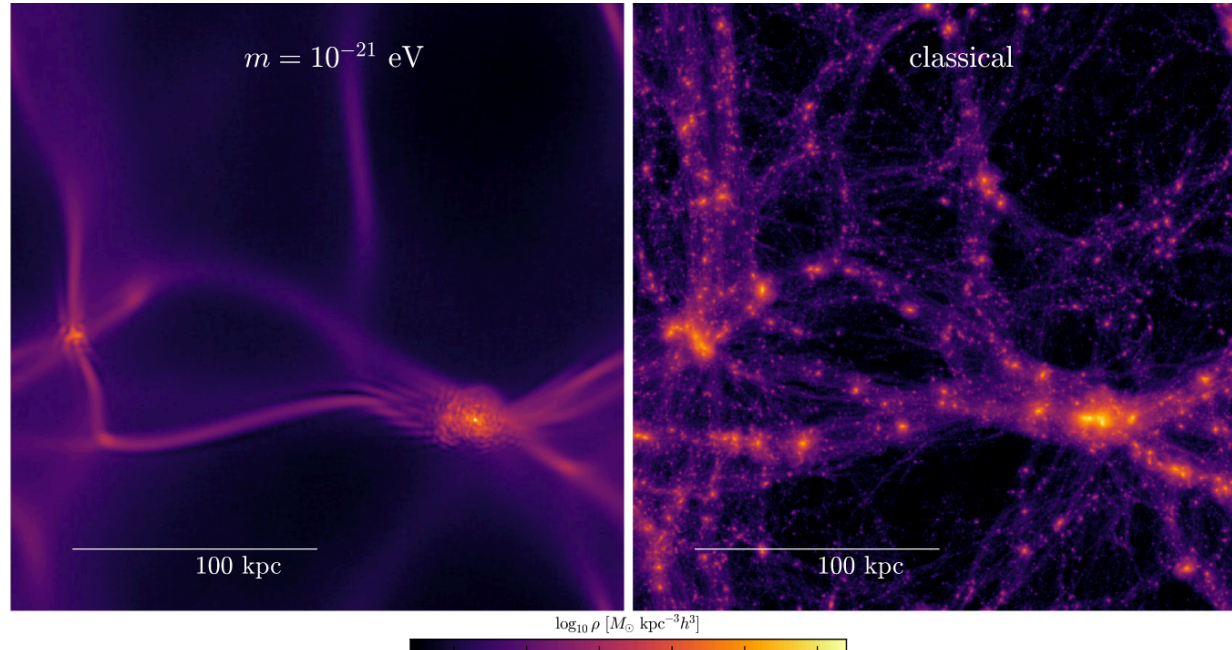
Density profiles observations and simulations

Antonino Popolo, Morgan Le Delliou (2017)

SFDM Motivation 2) Alternative to CDM N-Body simulations

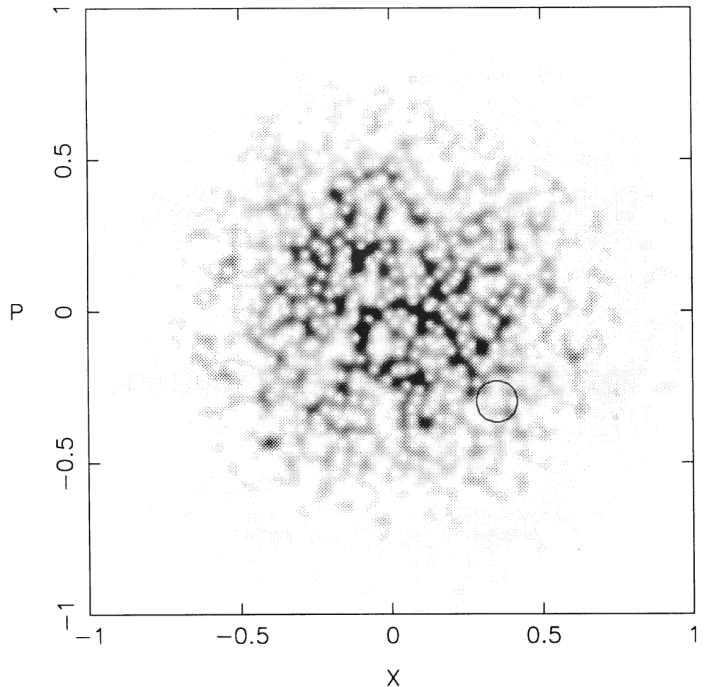
FDM comoving Vlasov equation

$$\frac{\partial f_W}{\partial t} + \frac{\vec{p}}{a^2} \cdot \frac{\partial f_W}{\partial \vec{x}} - \vec{\nabla}_x \varphi_N \cdot \frac{\partial f_W}{\partial \vec{p}} + \mathcal{O}(\epsilon) = 0.$$



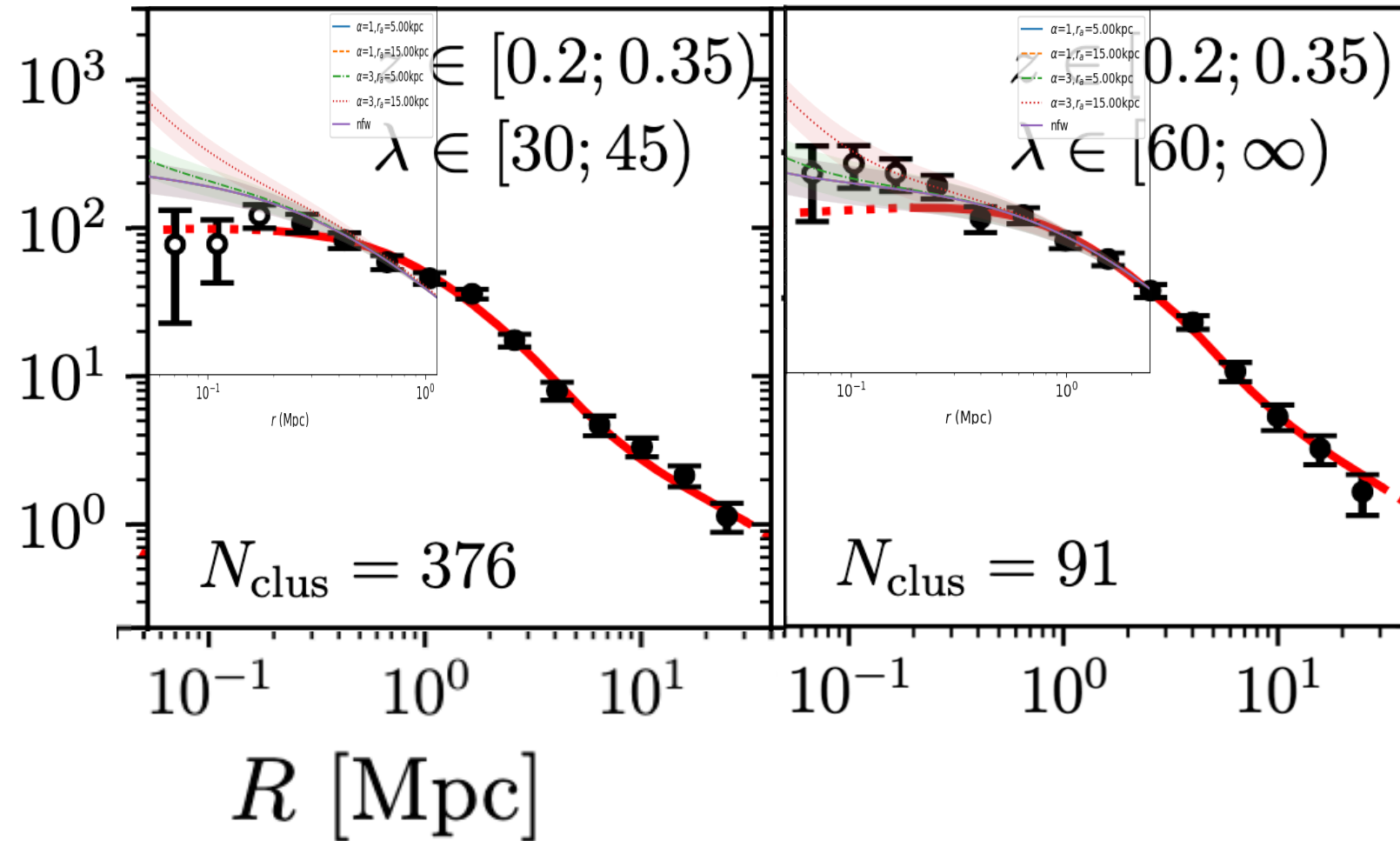
Cosmological simulation at $z=3$, evolved either as CDM (VP eq) or as FDM (SP)

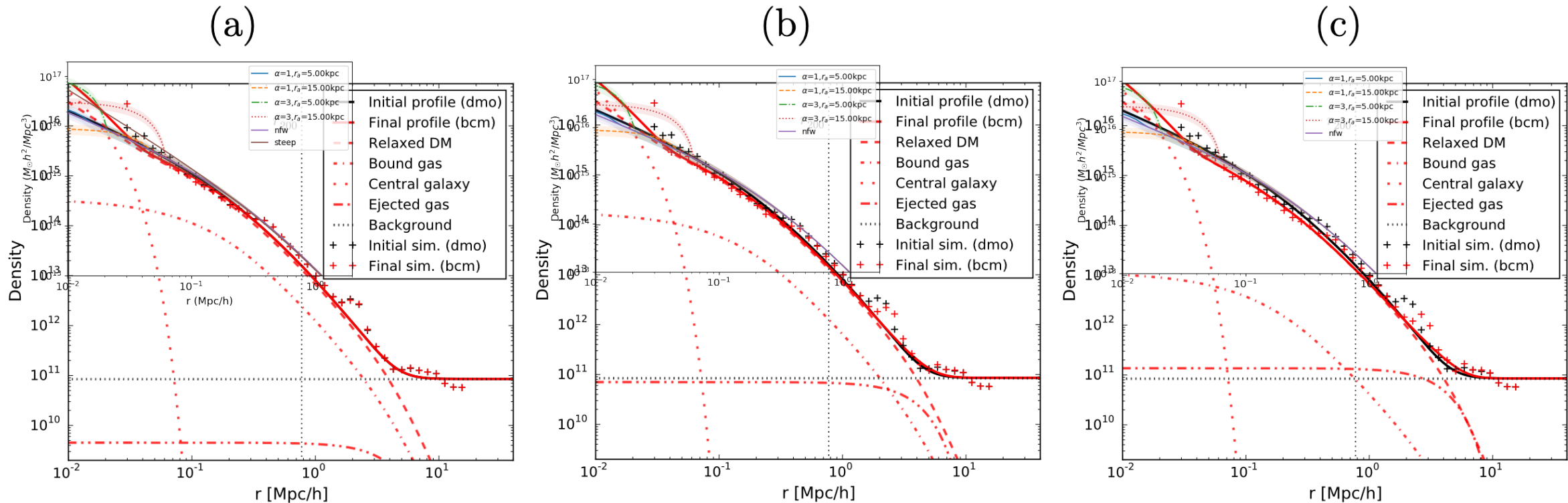
Philip Mocz and Lachlan Lancaste
Anastasia Fialkov and Fernando Becerra
Pierre-Henri Chavanis (2018).



Using Schrodinger equation to compute
collisionless cold dark mater
Kaiser (1993)

Summary and outlook



10^{**14} 

Self-interacting soliton

Soliton: Hydrostatic equilibrium

$$\Phi_N + \Phi_I + \Phi_Q = \alpha,$$

Thomas-Fermi regime $\rightarrow \Phi_Q \ll \Phi_I$

Soliton TF limit

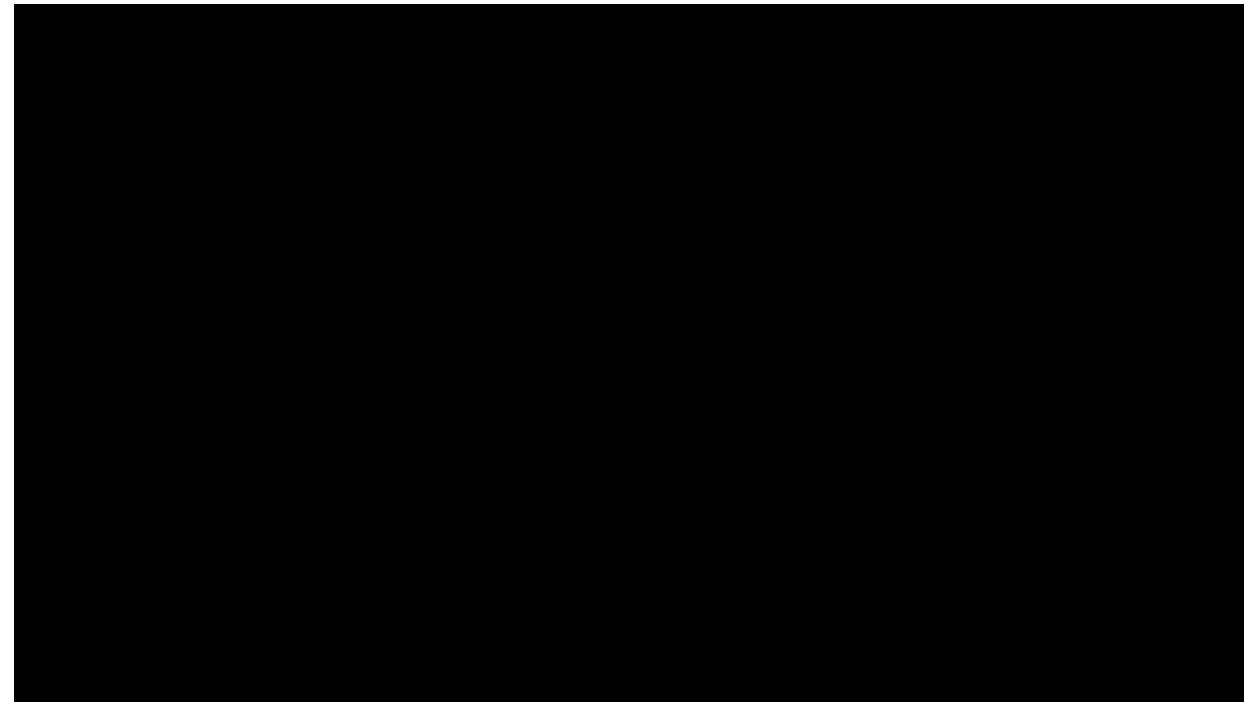
$$\Phi_N + \Phi_I = \alpha,$$

In this approximation, the soliton density profile :

$$\rho_{\text{sol}}(r) = \rho_{0\text{sol}} \frac{\sin(\pi r/R_{\text{sol}})}{\pi r/R_{\text{sol}}},$$

$$R_{\text{sol}} = \pi r_a, \text{ with } r_a^2 = \frac{3\lambda_4}{16\pi G_N m^4} :$$

r_a sets Jeans length !

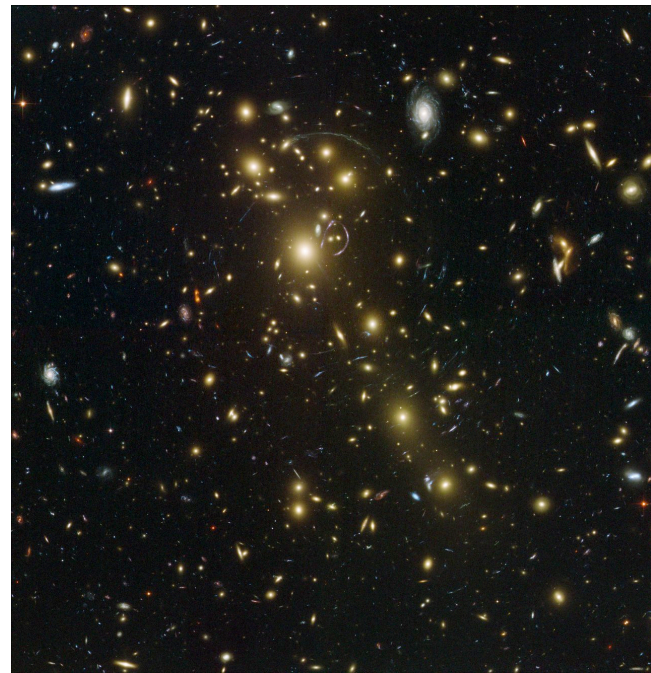


Flat halo with r_a of the order of the system

We consider the semi-classical limit, where λ_{dB} is smaller than both the core and halo radii.

R.Galazo-García et al. (2024)
acknowledgements to Jean Charles Lambert

Difference NFW - Soliton deflection angle



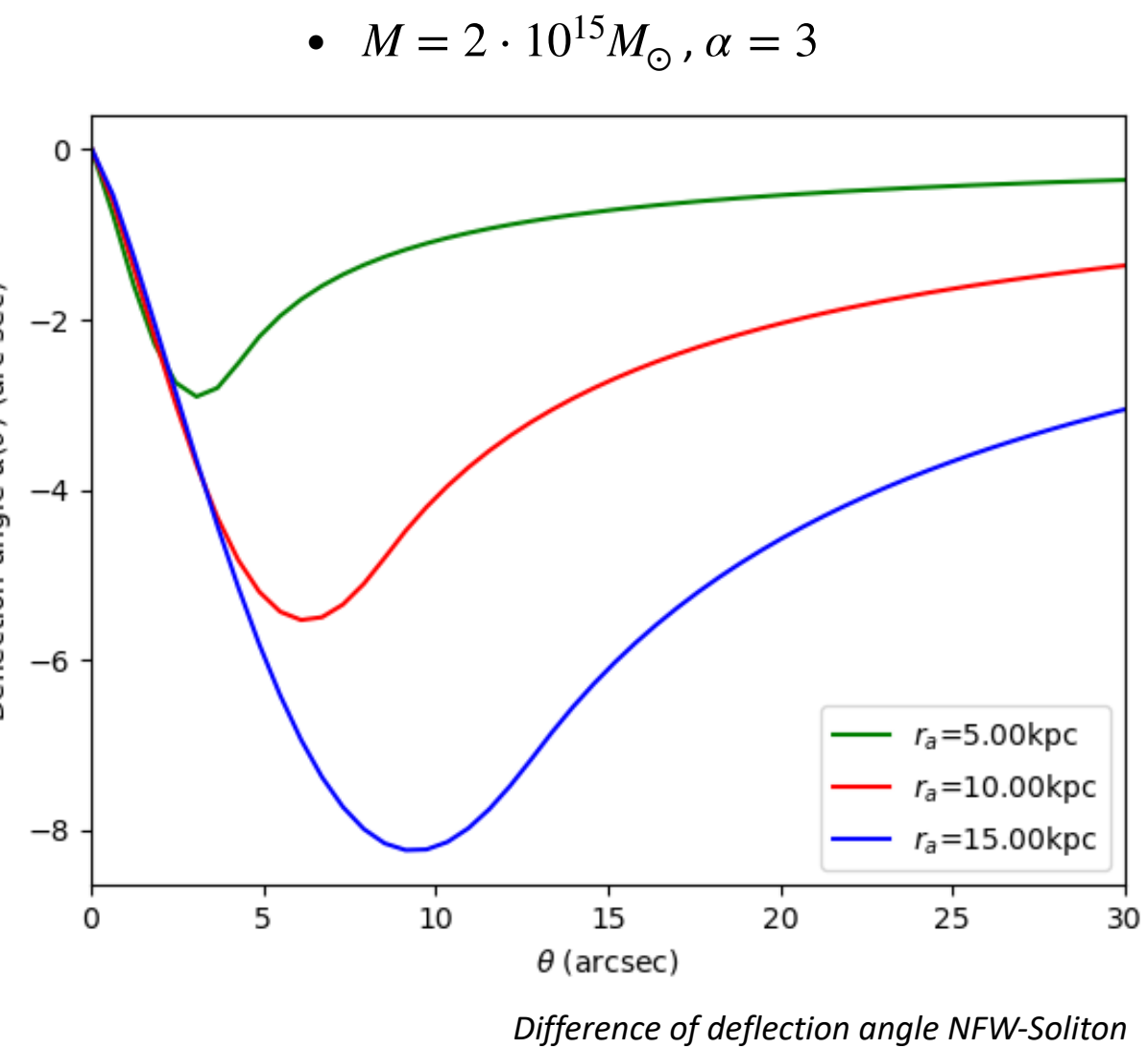
Abell 1709

Credit: NASA, ESA, and Johan Richard (Caltech, USA)

$$r_a = 5 \text{ kpc} \rightarrow \rho_c \sim 3.72 \cdot 10^8 M_\odot / \text{kpc}^3$$

$$r_a = 15 \text{ kpc} \rightarrow \rho_c \sim 1.17 \cdot 10^8 M_\odot / \text{kpc}^3$$

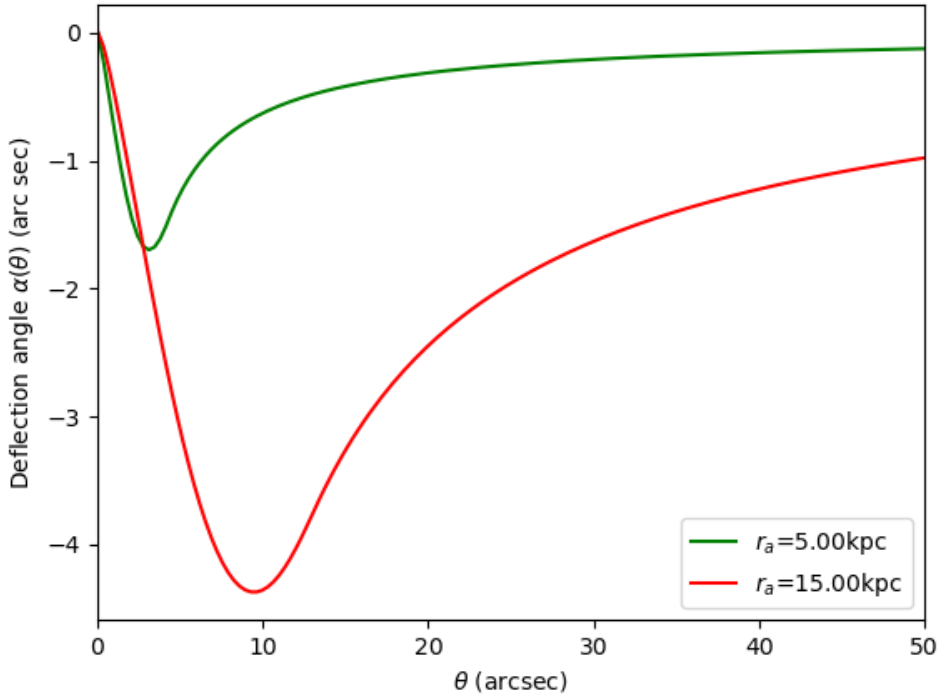
$$\text{NFW: } r_s = 800 \text{ kpc}, \rho_s \sim 5.77 \cdot 10^5 M_\odot / \text{kpc}^3$$



Soliton - Deflection angle and surface mass density

$\alpha = 3, r_a = 5\text{kpc}, r_t = 14\text{kpc}$

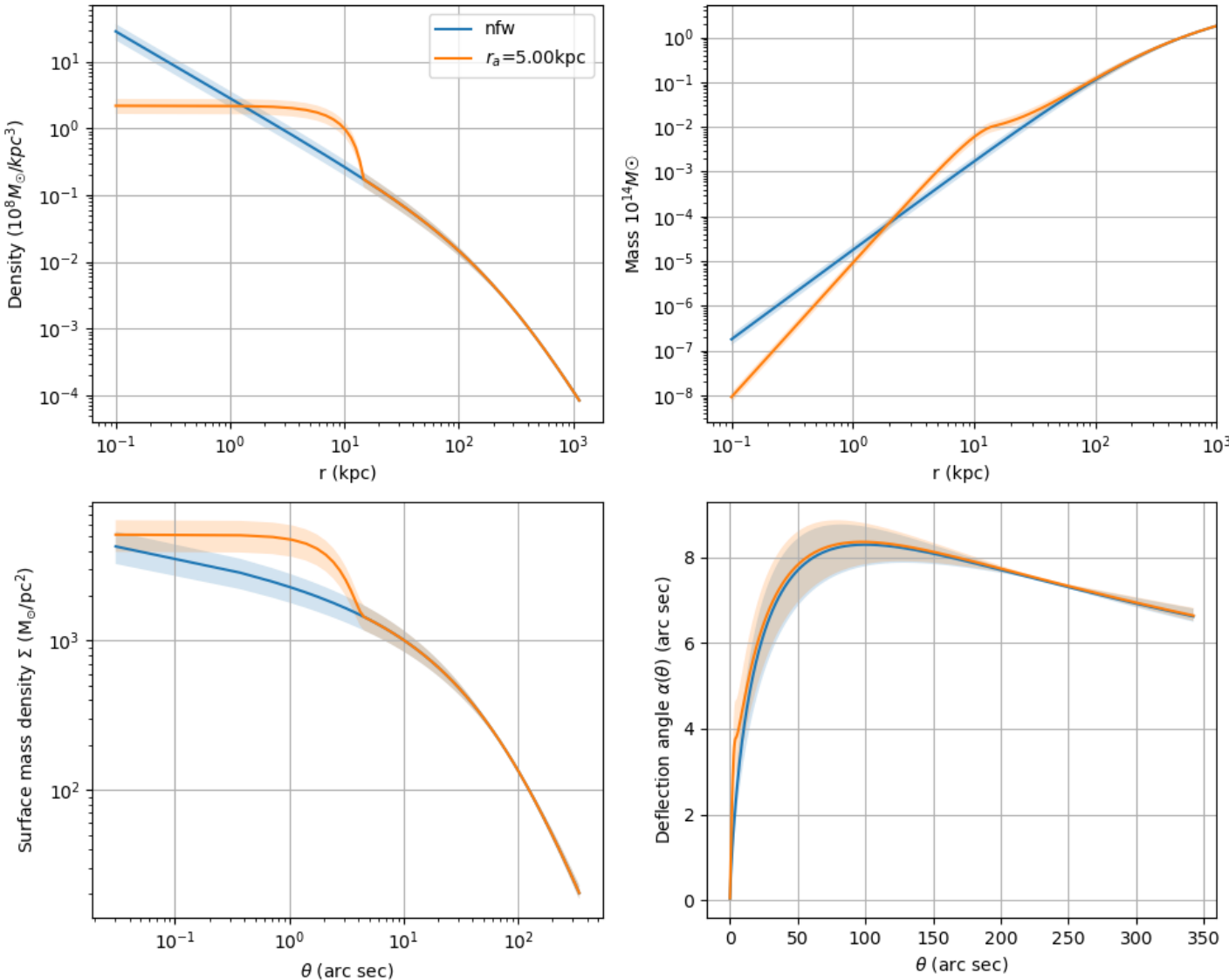
- $M = 2 \cdot 10^{14} M_\odot, \alpha = 3$



Difference of deflection angle NFW-Soliton

$$r_a = 5\text{kpc} \rightarrow \rho_c \sim 2.18 \cdot 10^8 M_\odot/\text{kpc}^3$$

$$r_a = 15\text{kpc} \rightarrow \rho_c \sim 6.30 \cdot 10^7 M_\odot/\text{kpc}^3$$



Self-interacting soliton

Soliton: Hydrostatic equilibrium

$$\Phi_N + \Phi_I + \Phi_Q = \alpha,$$

Thomas-Fermi regime $\rightarrow \Phi_Q \ll \Phi_I$

Soliton TF limit

$$\Phi_N + \Phi_I = \alpha,$$

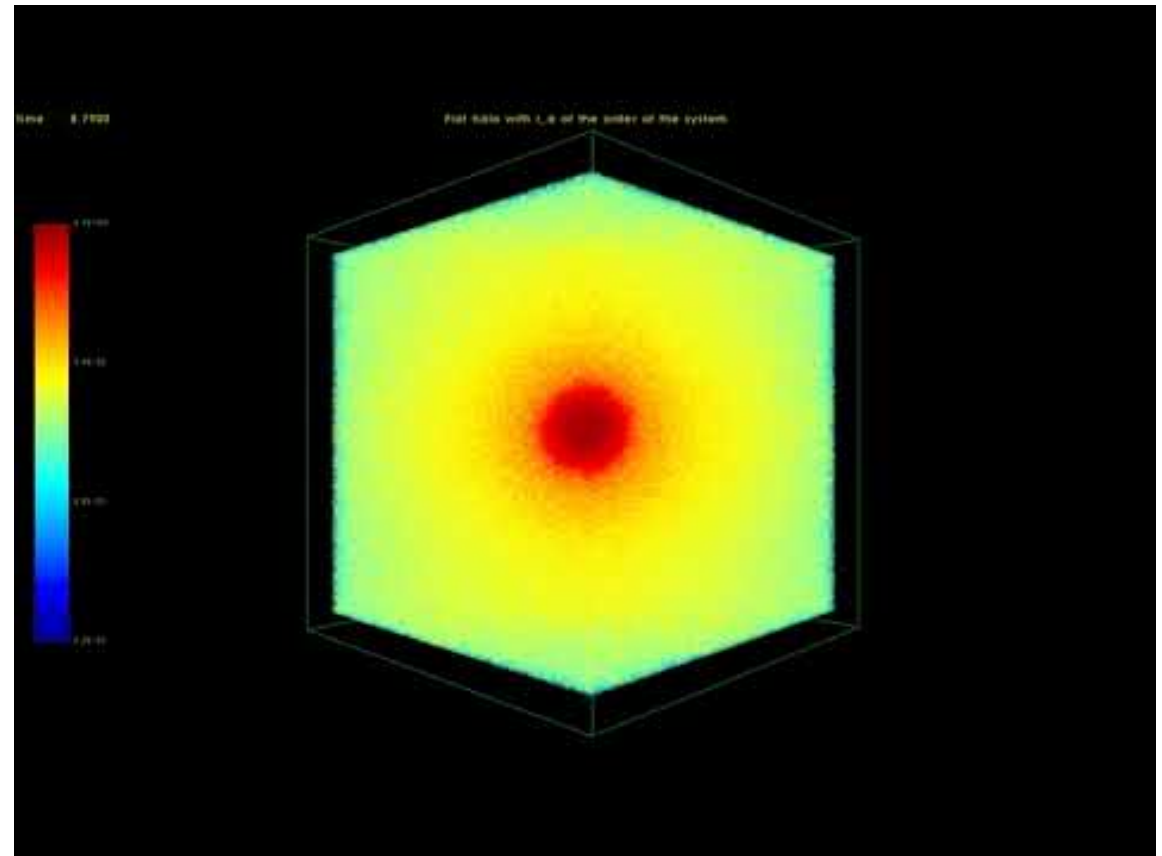
In this approximation, the soliton density profile :

$$\rho_{\text{sol}}(r) = \rho_{0\text{sol}} \frac{\sin(\pi r/R_{\text{sol}})}{\pi r/R_{\text{sol}}},$$

$$R_{\text{sol}} = \pi r_a, \text{ with } r_a^2 = \frac{3\lambda_4}{16\pi G_N m^4} :$$

r_a sets Jeans length !

We consider the semi-classical limit, where λ_{dB} is smaller than both the core and halo radii.



Flat halo with r_a of the order of the system

R.Galazo-García et al. (2024)
acknowledgements to Jean Charles Lambert

Self-interacting soliton

Soliton: Hydrostatic equilibrium

$$\Phi_N + \Phi_I + \Phi_Q = \alpha,$$

Thomas-Fermi regime $\rightarrow \Phi_Q \ll \Phi_I$

Soliton TF limit

$$\Phi_N + \Phi_I = \alpha,$$

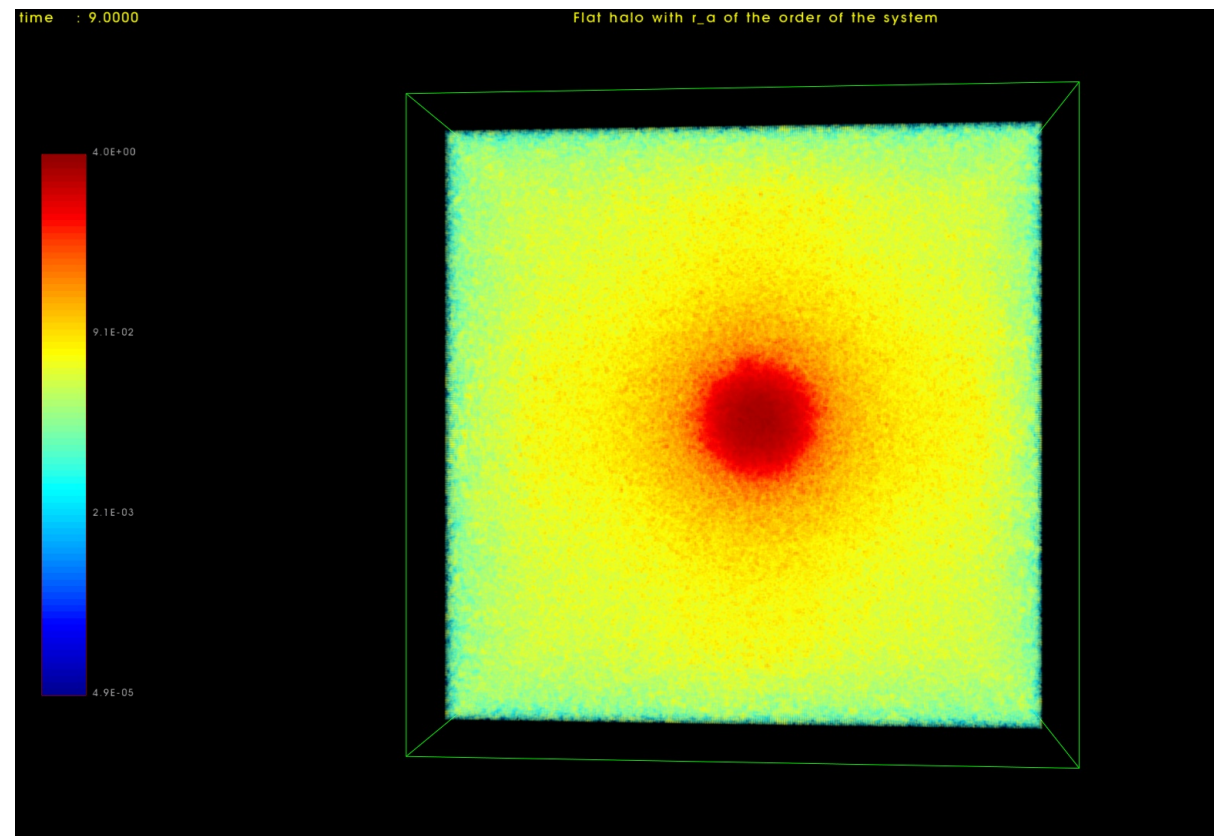
In this approximation, the soliton density profile :

$$\rho_{\text{sol}}(r) = \rho_{0\text{sol}} \frac{\sin(\pi r/R_{\text{sol}})}{\pi r/R_{\text{sol}}},$$

$$R_{\text{sol}} = \pi r_a, \text{ with } r_a^2 = \frac{3\lambda_4}{16\pi G_N m^4} :$$

r_a sets Jeans length !

We consider the semi-classical limit, where λ_{dB} is smaller than both the core and halo radii.



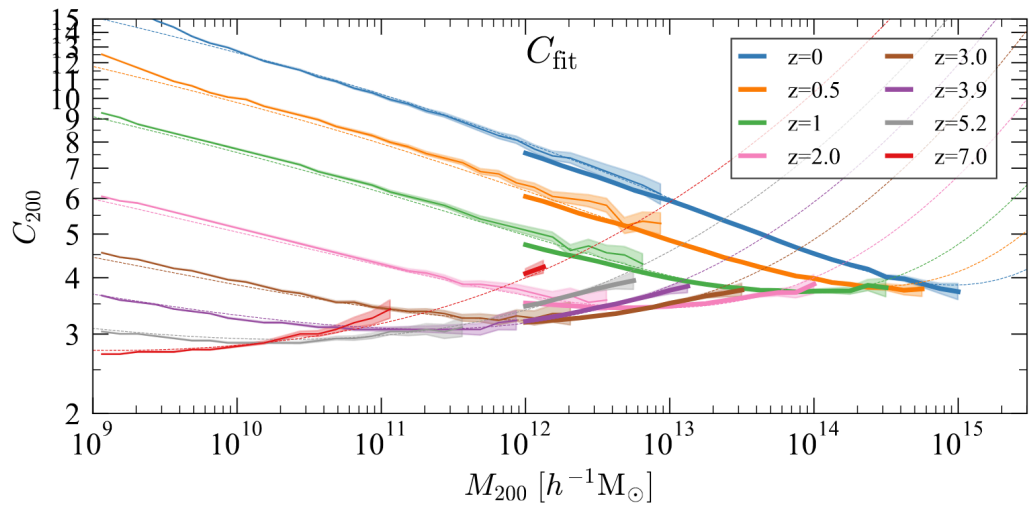
Flat halo with r_a of the order of the system

R.Galazo-García et al. (2024)
acknowledgements to Jean Charles Lambert

NFW - Deflection angle and surface mass density

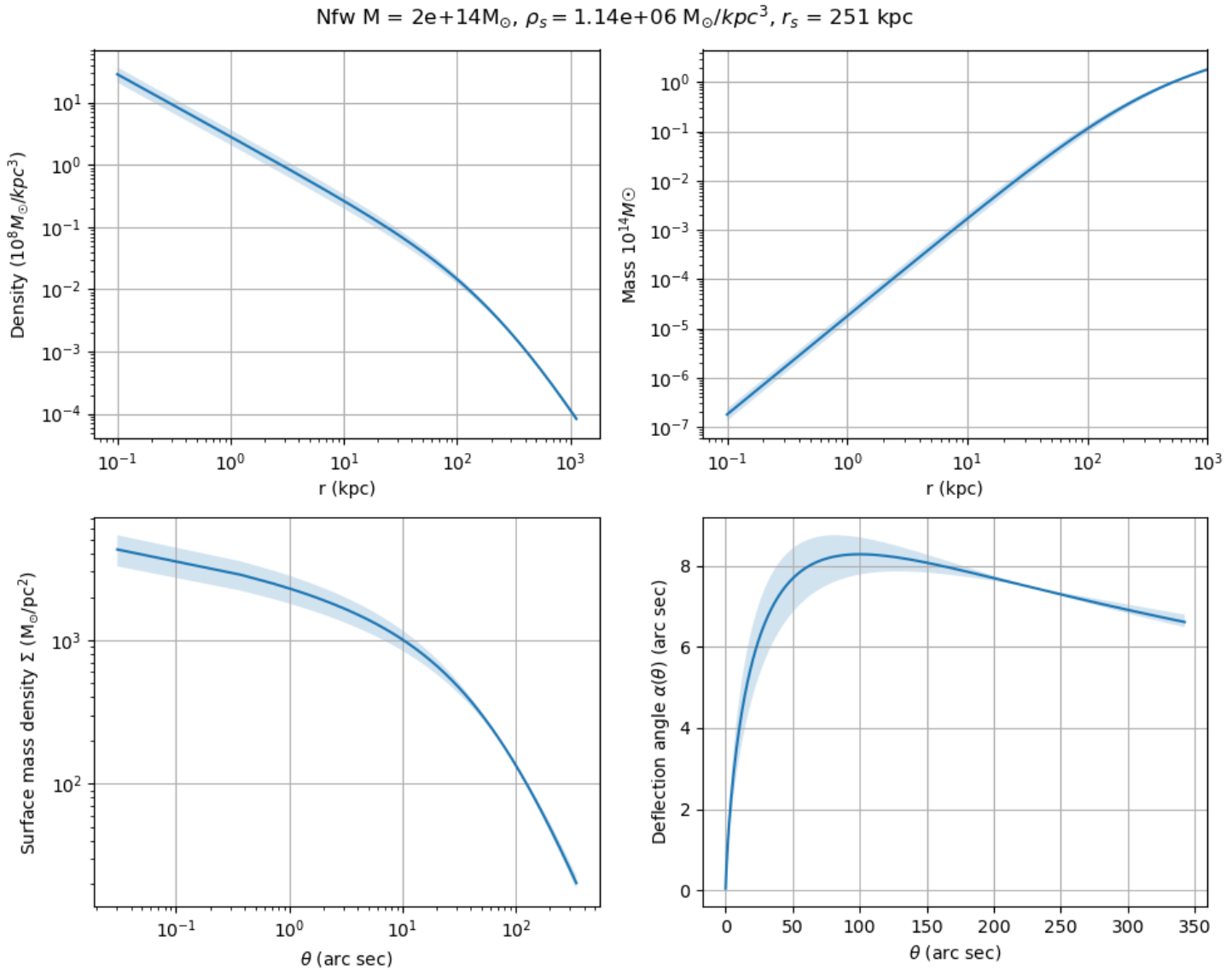
Galaxy Groups in the SL2S

- We build the NFW from the total mass of the system (r_{200}) and the concentration (C_{200}), and we get ρ_s .



Mass-concentration relation of halos for the Uchuu simulation

Ishiyama et al. (2021)



Initial ψ_{halo} and WKB approximation

Objective: To build a target radial halo density profile with random initial conditions.

$$\psi_{\text{initial}} = \psi_{\text{sol}} + \psi_{\text{halo}}.$$

Initial halo wavefunction:

$$\psi_{\text{halo}}(\vec{x}, t) = \sum_{n\ell m} a_{n\ell m} \hat{\psi}_{n\ell m}(\vec{x}) e^{-iE_{n\ell}t/\epsilon},$$

Eigenmodes of the Schrödinger eq. in the presence of the Φ_N due to the halo. (Spherical harmonics – time independent.)

The coefficients of the eigenmodes: $a_{n\ell m} = a(E_{n\ell}) e^{i\Theta_{n\ell m}},$

Uncorrelated random phases.

Amplitude: deterministic function of the energy.
Occupation numbers.

$$\langle \rho_{\text{halo}} \rangle = \sum_{n\ell m} a(E_{n\ell})^2 |\hat{\psi}_{n\ell m}|^2 \quad \langle \rho_{\text{halo}} \rangle = \bar{\rho},$$

Semi-classical regime -> WKB valid

- We choose the target density profile $\bar{\rho}$, and we compute $f(E)$: $\longrightarrow f(E) = \frac{1}{2\sqrt{2\pi^2}} \frac{d}{dE} \int_E^0 \frac{d\Phi_N}{\sqrt{\Phi_N - E}} \frac{d\rho_{\text{classical}}}{d\Phi_N}.$
- We determine the eigenmode coefficients $a(E)$ with $f(E)$: $\longrightarrow a(E)^2 = (2\pi\epsilon)^3 f(E). \quad a_{n\ell m} = a(E_{n\ell}) e^{i\Theta_{n\ell m}},$
- We determine the initial halo wavefunction: $\longrightarrow \psi_{\text{halo}}(\vec{x}, t) = \sum_{n\ell m} a_{n\ell m} \hat{\psi}_{n\ell m}(\vec{x}) e^{-iE_{n\ell}t/\epsilon},$

The WKB approximation is only used for the determination of the **initial eigenmodes coefficients**.
We solve explicitly the time-independent Schrödinger equation.

Numerical method

$$i\epsilon \frac{\partial \tilde{\psi}}{\partial \tilde{t}} = -\frac{\epsilon^2}{2} \tilde{\nabla}^2 \tilde{\psi} + (\tilde{\Phi}_N + \tilde{\Phi}_I) \tilde{\psi},$$

$$\tilde{\nabla}^2 \tilde{\Phi}_N = 4\pi \tilde{\rho},$$

Dimensionless Schrödinger-Poisson system

Integrating Schrödinger eq.



$$\psi(\vec{x}, t + \Delta t) = \exp \left[i \int_t^{t + \Delta t} dt' \left(\frac{\epsilon}{2} \nabla^2 - \frac{1}{\epsilon} \Phi \right) \right] \psi(\vec{x}, t), \quad \text{with } \Phi = \Phi_N + \Phi_I.$$

Trapezoidal rule for Φ & splitting the exp.



$$\psi(\vec{x}, t + \Delta t) \approx \exp \left[-i \frac{\Delta t}{2\epsilon} \Phi(\vec{x}, t + \Delta t) \right] \exp \left[i \frac{\Delta t \epsilon}{2} \nabla^2 \right] \exp \left[-i \frac{\Delta t}{2\epsilon} \Phi(\vec{x}, t) \right] \psi(\vec{x}, t).$$

Diagonal in configuration space

Diagonal in Fourier space

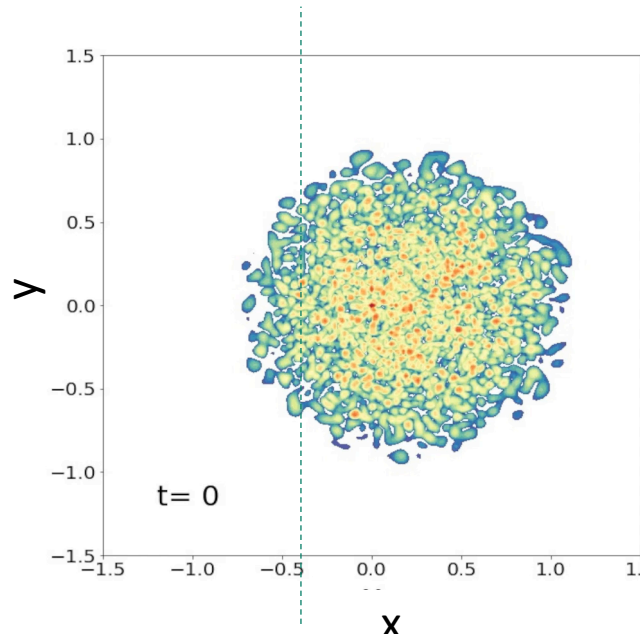
$$\psi(\vec{x}, t + \Delta t) = \exp \left[-\frac{i\Delta t}{2\epsilon} \Phi(\vec{x}, t + \Delta t) \right] \mathcal{F}^{-1} \exp \left[-\frac{i\epsilon\Delta t}{2} k^2 \right] \mathcal{F} \exp \left[-\frac{i\Delta t}{2\epsilon} \Phi(\vec{x}, t) \right] \psi(\vec{x}, t).$$

$$\Phi_N(\vec{x}, t + \Delta t) = \mathcal{F}^{-1} \left(-\frac{4\pi}{k^2} \right) \mathcal{F} |\psi|^2$$



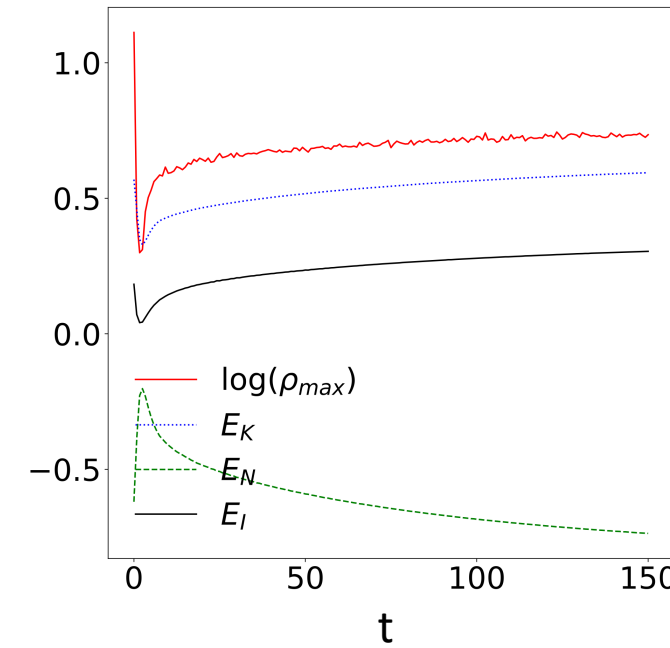
I) Flat halo with r_a of the order of the system

Density slice 2D (x, y) at $z=r_{max}, (\rho_{max})$

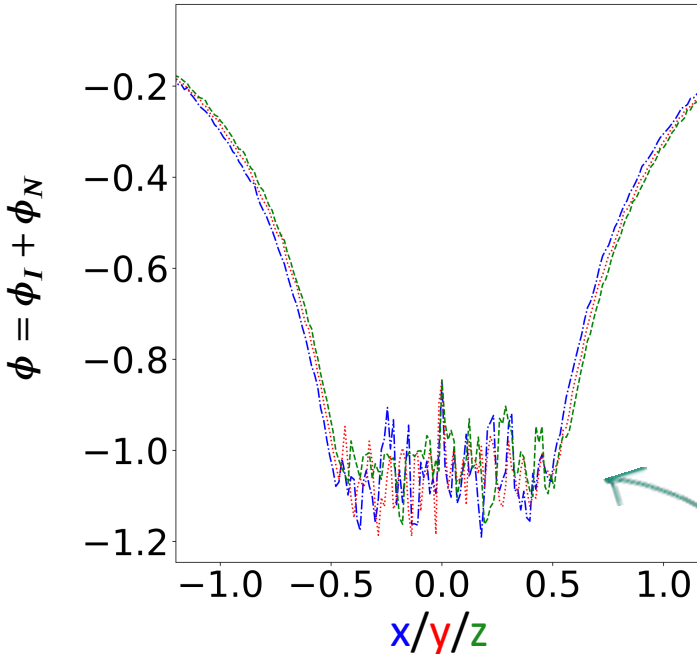


$$R_{sol} = \frac{\sqrt{\lambda\pi}}{2} = 0.5$$

$\rho_{max}, E_K, E_I, E_N$



Potential at $t=150$

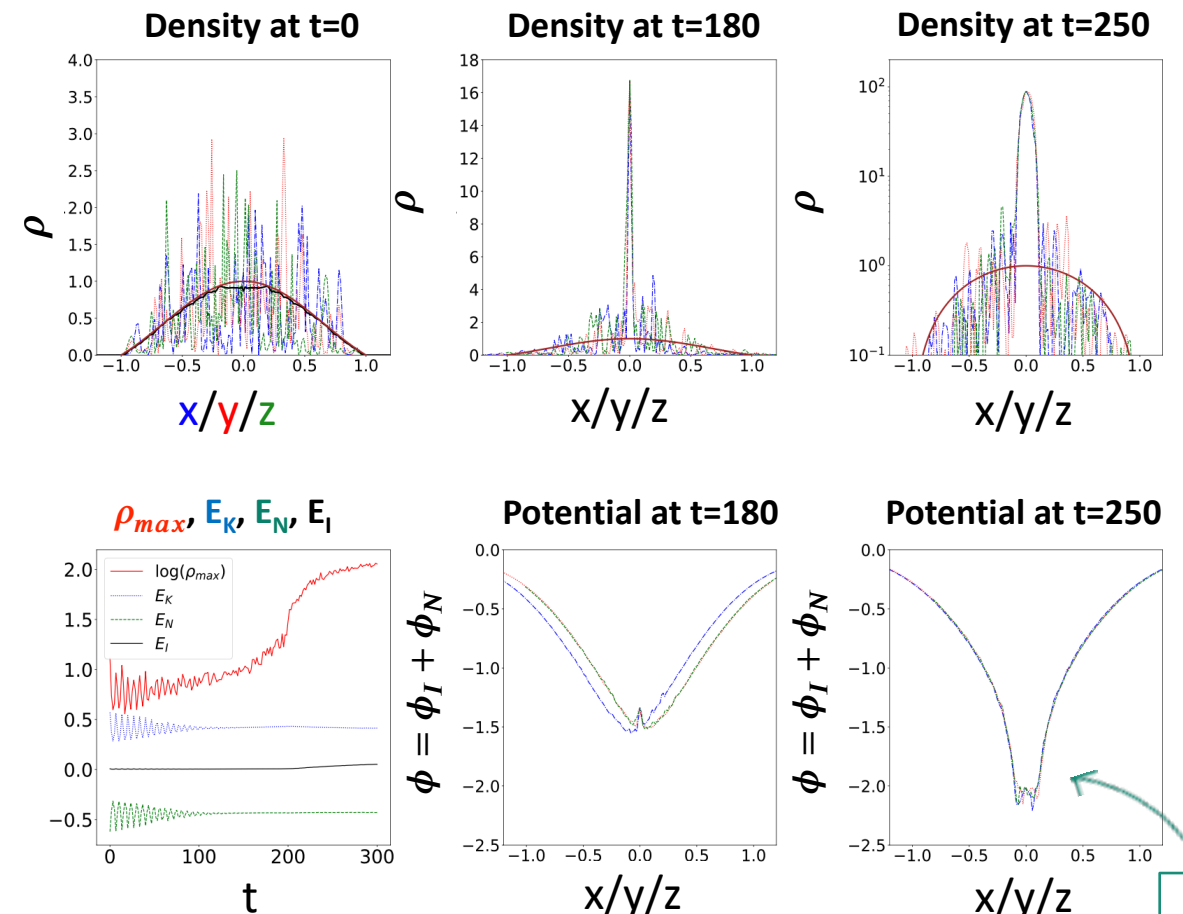
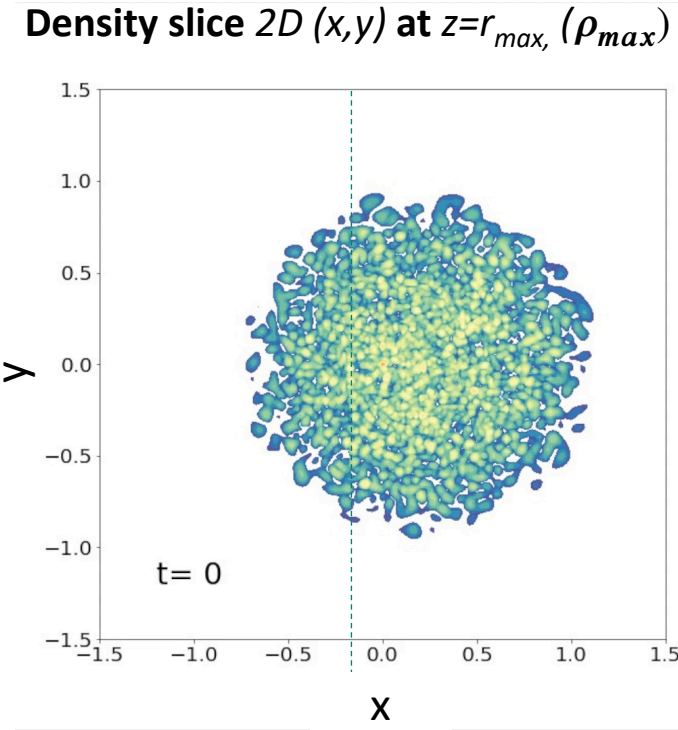


Soliton

$$\Phi_N + \Phi_I = \alpha,$$

- At $t \sim 8$, the soliton is formed with $R_{sol} = 0.5$ and contains about 40% of the total mass.
- The system reaches a quasi-stationary state.
- Afterwards, ρ_{max} and the energies only show a slow evolution.

II) Flat halo with r_a much smaller than system



- By $t \sim 100$, the halo relaxes to a quasi-stationary state.
- At $t \sim 180$, FDM peak.
- At $t \sim 200$, self-interacting soliton forms, $R_{sol} = 0.1$.

Transition from a **FDM phase** to a **self-interacting phase**.

Kinetic theory

- Simple kinetic equations: the **interplay between smooth background and stochastic fluctuations.**
- Focuses on occupation numbers of central soliton and halo eigenstates.
- **Effects of self-interactions and non-homogeneous background** ->decompose into eigenmodes of reference potential, similar to halo description.
- Importance of distinguishing smooth background from stochastic fluctuations: Fluctuations introduce randomness and are crucial in system's evolution.

$$i\epsilon \frac{\partial \psi}{\partial t} = -\frac{\epsilon^2}{2} \nabla^2 \psi + \Phi \psi,$$

$$\Phi = (4\pi \nabla^{-2} + \lambda) \psi^* \psi.$$

If the Φ is fixed, $\psi(\vec{x}, t)$ can be decomposed as usual in energy eigenmodes with the simple time dependence. $e^{-iEt/\epsilon}$.

Dimensionless Schrödinger-Poisson system

We focus on an effective model of scalar dark matter that remains valid below a specific cut-off energy scale, denoted as Λ

where $V_I(\phi)$ is the self-interaction potential,

$$V_I(\phi) = \Lambda^4 \sum_{n \geq 3} \frac{\lambda_p}{p} \frac{\phi^p}{\Lambda^p}.$$

$$\phi = \frac{1}{\sqrt{2m}}(\psi e^{-imt} + \psi^* e^{imt}), \quad (2.33)$$

This allows us to separate the fast oscillations at frequency $m \sim (3 \text{ months})^{-1}$ from the slower dynamics described by ψ that follow the evolution of the density field and of the gravitational potential. Note that the complex scalar field ψ also satisfies the slow varying conditions (2.28)-(2.29), that is, $\dot{\psi} \ll m\psi$ and $\nabla\psi \ll m\psi$. Replacing (2.33) into the Klein-Gordon equation for ϕ (2.31) leads to the Schrödinger equation for ψ ,

$$i\frac{\partial\psi}{\partial t} = -\frac{1}{2m}\nabla^2\psi + m\Phi_N\psi + \frac{\partial\mathcal{V}_I}{\partial\psi^*}, \quad (2.34)$$

where now Φ_N is the gravitational potential. Note that we have changed the notation from $\Phi \rightarrow \Phi_N$. The self-interaction potential, denoted as $\mathcal{V}_I(\psi, \psi^*)$ is derived by replacing the decomposition (2.33) in the definition of $V_I(\phi)$, (2.3). We selectively keep only the non-oscillatory terms. This implies that in the series expansion (2.3), we exclusively consider the even order terms ϕ^{2n} , where each n factor of e^{-imt} is paired with n factors of e^{imt} . Consequently, the resulting expression is:

$$\mathcal{V}_I(\psi, \psi^*) = \Lambda^4 \sum_{n=2} \frac{\lambda_{2n}}{2n} \frac{(2n)!}{(n!)^2} \left(\frac{m\psi\psi^*}{2m\Lambda^2} \right)^n. \quad (2.35)$$

Next, let us define the following self-interaction potential to make the Schrödinger equation (2.34) more user-friendly,

$$\Phi_I(\rho) = \frac{d\mathcal{V}_I}{d\rho}, \quad (2.36)$$

where ρ is the ultra-light scalar density,

$$\rho = m\psi\psi^*. \quad (2.37)$$

Field picture

- Relativistic regime + FLRW background:

$$\ddot{\phi} + 3H(t)\dot{\phi} + \frac{dV(\phi)}{d\phi} = 0,$$

- The Einstein-Klein Gordon system.
- The non-relativistic regime relevant for structure formation, it is useful to introduce a complex scalar ψ

$$\phi = \frac{1}{\sqrt{2ma^3}}(\psi e^{-imt} + \psi^* e^{imt}),$$

$$\left| \ddot{\psi} \right| \ll m \left| \dot{\psi} \right| \quad \text{Factor-out the fast time oscillation of } \phi$$

Field picture: Schrodinger—Poisson system (SP)

The equations of motion of the action yield the Nonlinear Schrödinger—Poisson system:

$$i\dot{\psi} = -\frac{3}{2}iH\psi - \frac{1}{2ma^2}\nabla^2\psi + m(\Phi_N + \Phi_I),$$

$$\nabla^2\Phi_N = 4\pi Gma^2|\psi|^2.$$

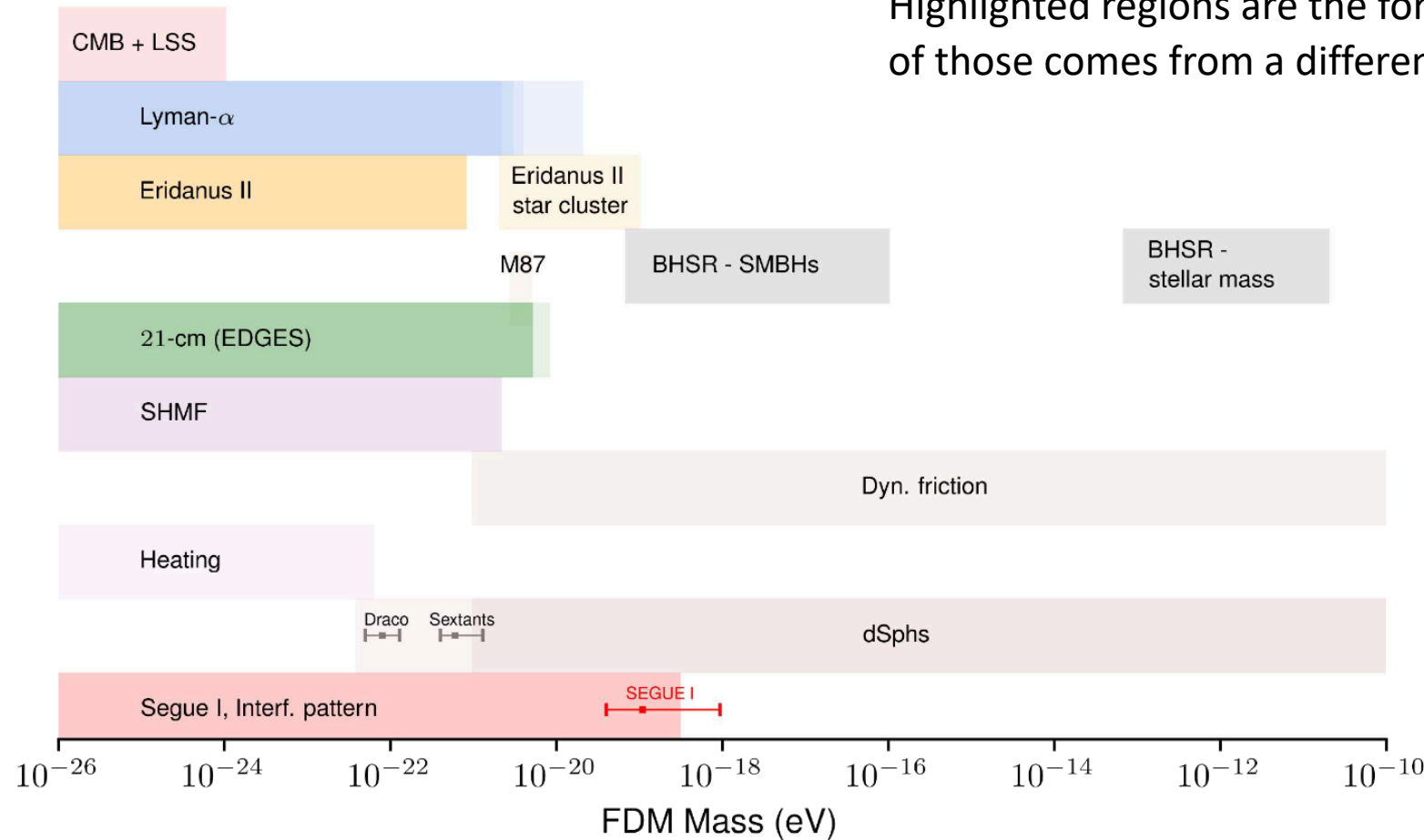
At small-scales, expansion of the universe is negligible:

$$i\frac{\partial\psi}{\partial t} = -\frac{1}{2m}\nabla^2\psi + m(\Phi_N + \Phi_I)\psi,$$

$$\nabla^2\Phi_N = 4\pi\mathcal{G}_N\rho.$$

$$\rho = m\psi\psi^*.$$

Mass limits



Highlighted regions are the forbidden regions for the mass each of those comes from a different observation

Cosmological evolution

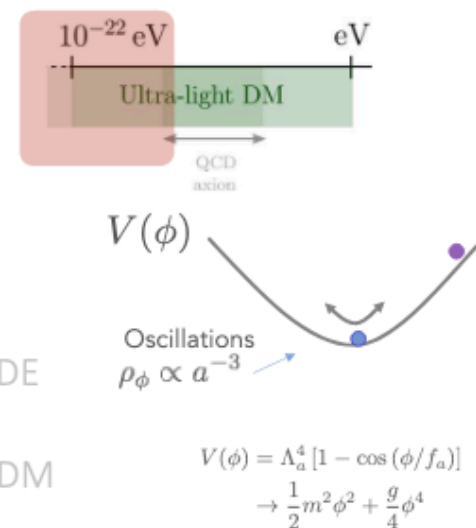
Cosmological evolution

Slide: Elisa M Ferreira

Cosmology from home
2022

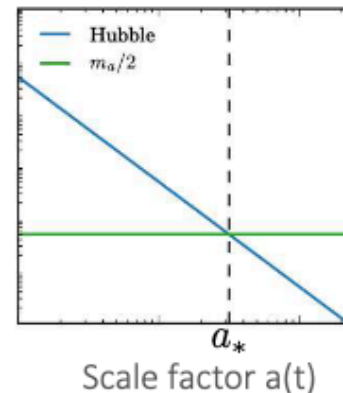
$$\ddot{\phi} + 3H\dot{\phi} + m^2\phi = 0$$

FDM

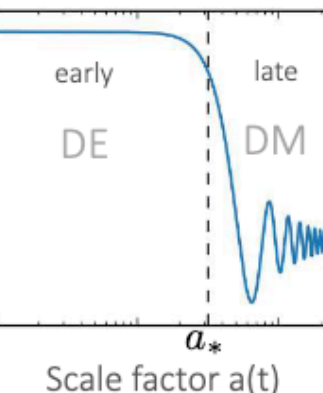


$$\begin{cases} H \gg m & \Rightarrow \phi_{\text{early}} = \phi(t_i) \rightarrow \omega = -1 \\ H \ll m & \Rightarrow \phi_{\text{late}} \propto e^{imt} \rightarrow \langle \omega \rangle = 0 \end{cases}$$

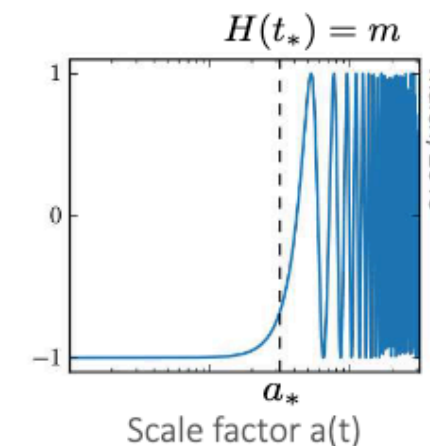
DE DM



UL field



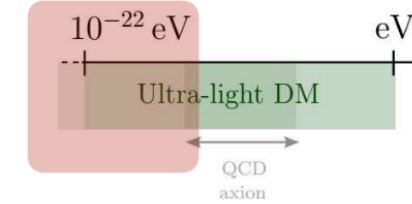
Scale factor $a(t)$



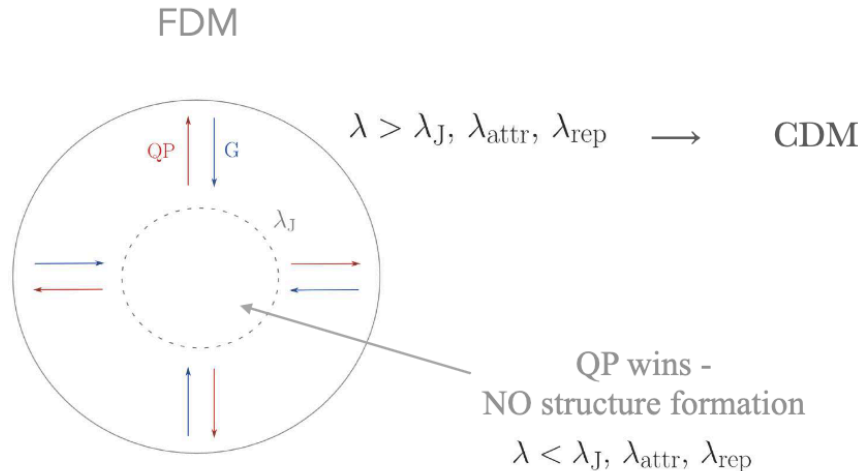
Scale factor $a(t)$

In order to behave like DM: start oscillating before matter-radiation equality $m > 10^{-28} \text{ eV} \sim H(a_{\text{eq}})$

Structure formation - perturbation and stability



Finite clustering scale - no structure formation on small scales



Finite size coherent core – Bose stars

$$\lambda_J = 55 \left(\frac{m}{10^{-22} \text{ eV}} \right)^{-1/2} \left(\frac{\rho}{\bar{\rho}} \right)^{-1/4} (\Omega_m h)^{-1/4} \text{ kpc}$$

$m \leq 10^{-20} \text{ eV} \Rightarrow \lambda_{dB} > \mathcal{O}(\text{kpc})$ Galactic scales

$$\dot{\rho} + \nabla \cdot (\rho \mathbf{v}) = 0$$

$$\dot{\mathbf{v}} + (\mathbf{v} \cdot \nabla) \mathbf{v} = -\frac{1}{m} \left(V_{\text{grav}} - P_{\text{int}} - \frac{1}{2m} \frac{\nabla^2 \sqrt{\rho}}{\sqrt{\rho}} \right)$$

↑ $P_{\text{int}} = \frac{g}{2m^2} \rho^2$

 $\frac{1}{2m} \frac{\nabla^2 \sqrt{\rho}}{\sqrt{\rho}}$

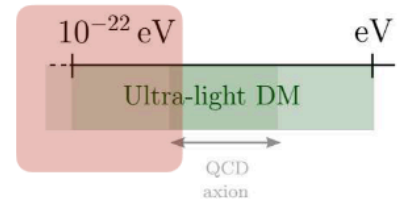
→ Quantum pressure

Slide: Elisa M Ferreira
Cosmology from home
2022

Phenomenology

Suppression of small structures

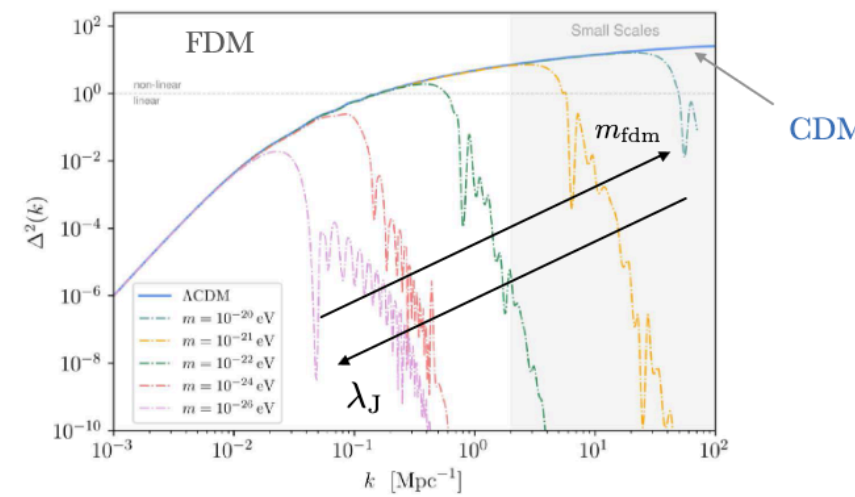
Slide: Elisa M Ferreira
Cosmology from home 2022



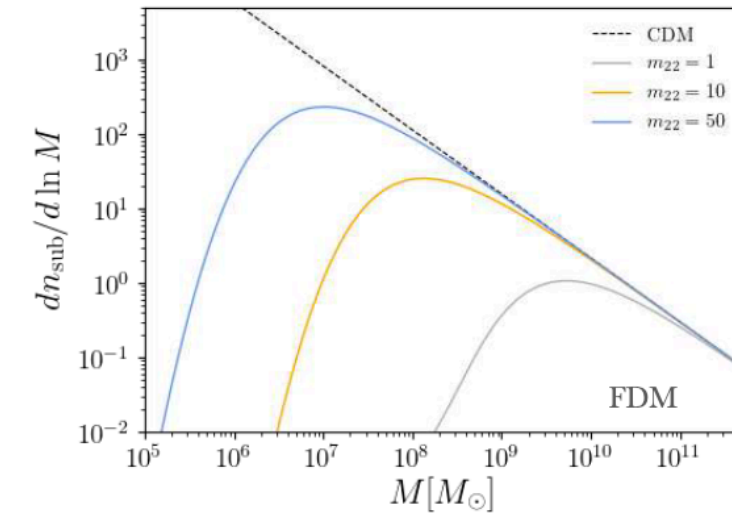
Finite Jeans length λ_J or $\lambda_{attr}, \lambda_{rep}$

Suppresses small scale structure

POWER SPECTRUM



(sub) HALO MASS FUNCTION



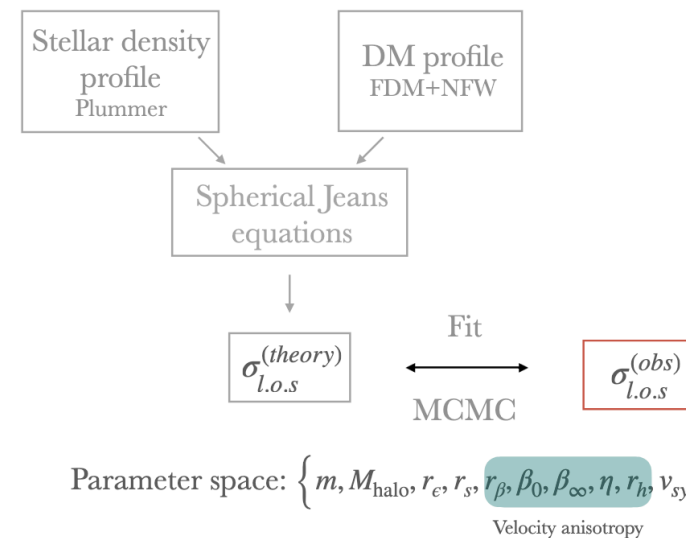
Ultra-light Dark Matter FDM mass from Ultra-faint dwarfs

Slide: Elisa M Ferreira
Cosmology from home 2022

Hayashi, E.F,Chan, 2021.

Ultra-faint dwarfs (UFD): ideal laboratory to study DM

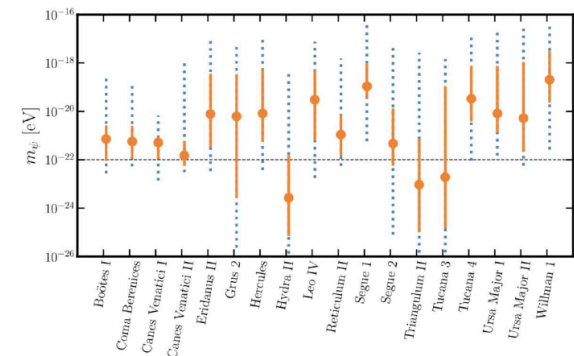
Stellar kinematic data from 18 UFDs to fit the FDM profile



$$\rho(r) = \begin{cases} \rho_{\text{soliton}} \simeq \frac{\rho_c}{[1 + 0.091(r/r_c)^2]^8}, & r < r_c \\ \rho_{\text{NFW}} = \frac{\rho_s}{(r/r_s)(1+r/r_s)^2}, & r > r_c \end{cases}$$

$$\rho_c(r) = 1.9 \times 10^{12} \left(\frac{m}{10^{-23} \text{ eV}} \right)^{-2} \left(\frac{r_c}{\text{pc}} \right)^{-4} [M_\odot \text{ pc}]$$

$$r_c \simeq 1600 \left(\frac{m}{10^{-23} \text{ eV}} \right)^{-1} \left(\frac{M_{\text{halo}}}{10^{12} M_\odot} \right)^{-1/3} [\text{pc}]$$

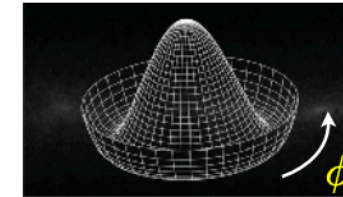


Strongest constraint on m_{FDM} to date!

Particle physics motivations

- A natural candidate for a light (scalar) particle is a pseudo-Nambu-Goldstone boson.

A well known example is the QCD axion (Peccei, Quinn; Weinberg; Wilczek; Kim; Shifman, Vainshtein, Zakharov, Zhitnitsky; Dine, Fischler, Srednicki; Preskill, Wise, Wilczek; Abbott, Sikivie).



There are also many axion-like-particles in string theory (Svrcek, Witten; Arvanitaki et al.)

Footnote on ultra-light version

mass $m \leftarrow 10^{-22} \text{ eV} \rightarrow$ Fuzzy dark matter (FDM)
Hu, Barkana, Gruzinov
Amendola, Barbieri

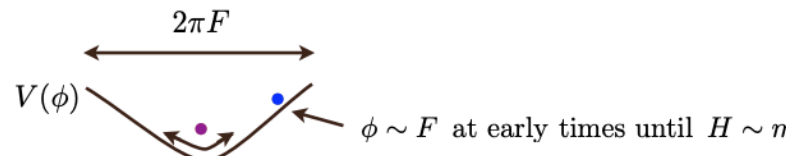
- Consider an angular field (a pseudo Nambu-Goldstone) of periodicity $2\pi F$ i.e. an axion-like field with a potential from non-perturbative effects (not QCD axion).

$$\mathcal{L} \sim -\frac{1}{2}(\partial\phi)^2 - \Lambda^4(1 - \cos[\phi/F])$$

$$m \sim \Lambda^2/F$$

(candidates: Arvanitaki et al.
Svrcek, Witten)

- Relic abundance matches dark matter abundance (mis-alignment mechanism).



$$\Omega_{\text{matter}} \sim 0.1 \left(\frac{F}{10^{17} \text{ GeV}} \right)^2 \left(\frac{m}{10^{-22} \text{ eV}} \right)^{1/2}$$

(Preskill, Wise, Wilczek; Abbott, Sikivie; Dine, Fischler, with constant m)

Slide: Lam Hui

Les Houches Summer School
2021

Experimental implications (light DM e.g. QCD axion):

$$\mathcal{L} \sim \frac{\phi}{f} F_{\mu\nu} \tilde{F}^{\mu\nu} + \frac{\partial_\mu \phi}{f} \bar{\Psi} \gamma^5 \gamma^\mu \Psi$$

Reviews: Sikivie 2003
Graham et al. 2015, Marsh 2016

- **Coupling to EM**

ADMX (cavity) - photon from axion in magnetic field

$$\phi^2$$

ABRACADABRA - magnetic flux from axion in magnetic field

$$\dot{\phi}$$

ADBC - rotation of polarization of photon propagating in axion

$$\Delta\phi$$

- **Coupling to spin** $\hat{H} \sim \vec{\nabla}\phi \cdot \hat{\sigma}$

CASPER - spin precession like in NMR

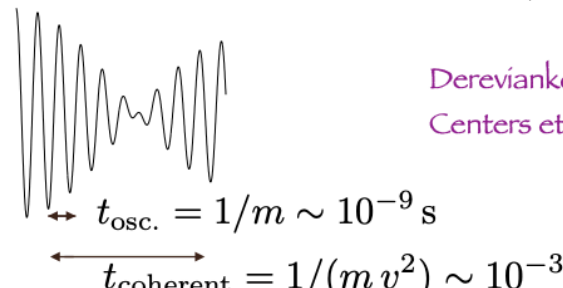
$$\vec{\nabla}\phi$$

Eot-Wash - torsional spin pendulum

$$\vec{\nabla}\phi$$

- $\phi \sim \psi e^{-imt} + \psi^* e^{imt}$

slow fast



Derevianko; Foster, Rodd, Safdi;
Centers et al.

- Measure correlation functions e.g.

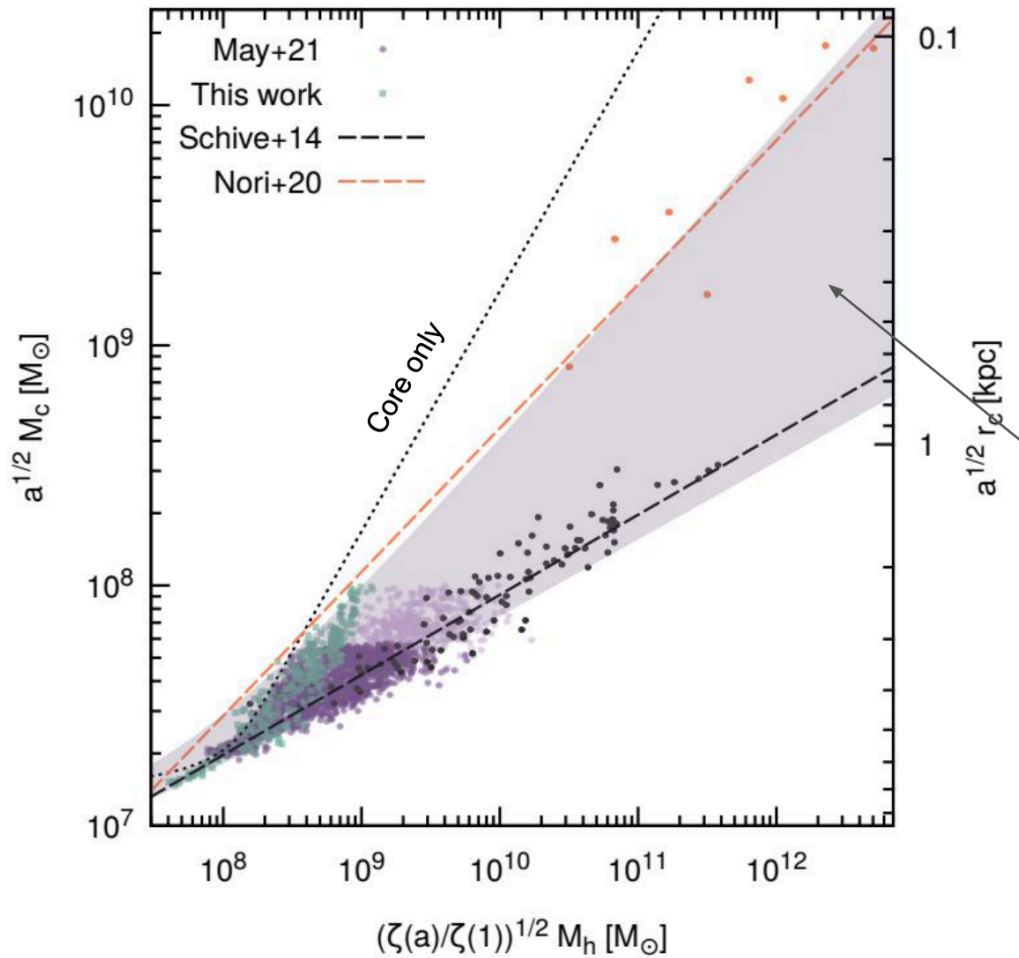
$$\langle \phi(t)^2 \phi(t')^2 \rangle - \langle \phi^2 \rangle^2 \sim [|t - t'|/t_{\text{coherent}}]^{-3} + \text{osc.} \quad (\text{or even space-time correlations}).$$

- At vortices $\phi = 0$ but $\vec{\nabla}\phi \neq 0$.

- Phase of oscillation might be interesting: $\phi \sim |\psi| \cos(mt - \theta)$.

Slide: Lam Hui

Les Houches Summer School
2021



- **Dispersion !**
- **Previous studies only describe part of the core-halo population**

- **New Empirical Equation**

$$M_c = \beta + (M_h/\gamma)^\alpha$$

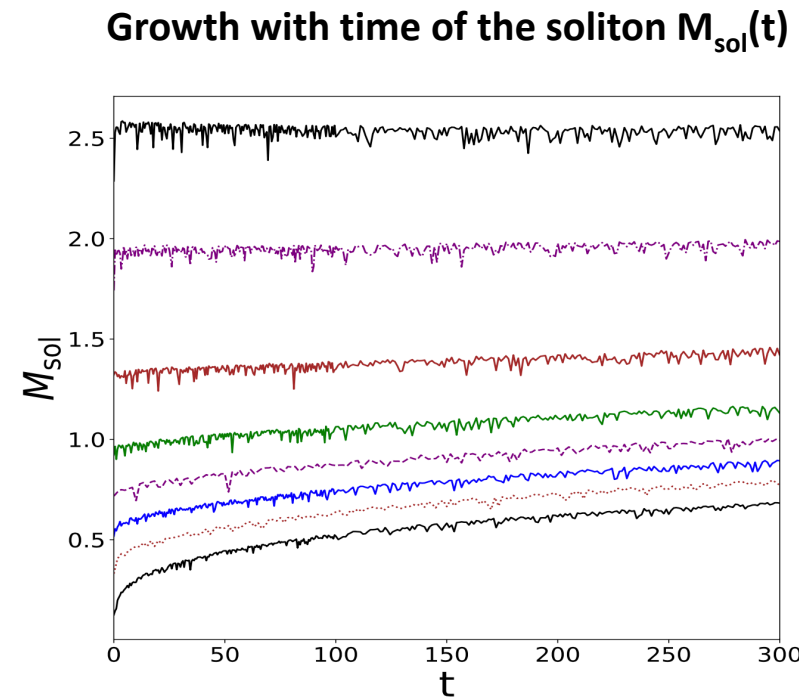
In Schive et al. (2014b), a fitting function for the core–halo mass relation was obtained:

$$M_c = \frac{1}{4\sqrt{a}} \left[\left(\frac{\zeta(z)}{\zeta(0)} \right)^{1/2} \frac{M_h}{M_{\min,0}} \right]^{1/3} M_{\min,0}, \quad (11)$$

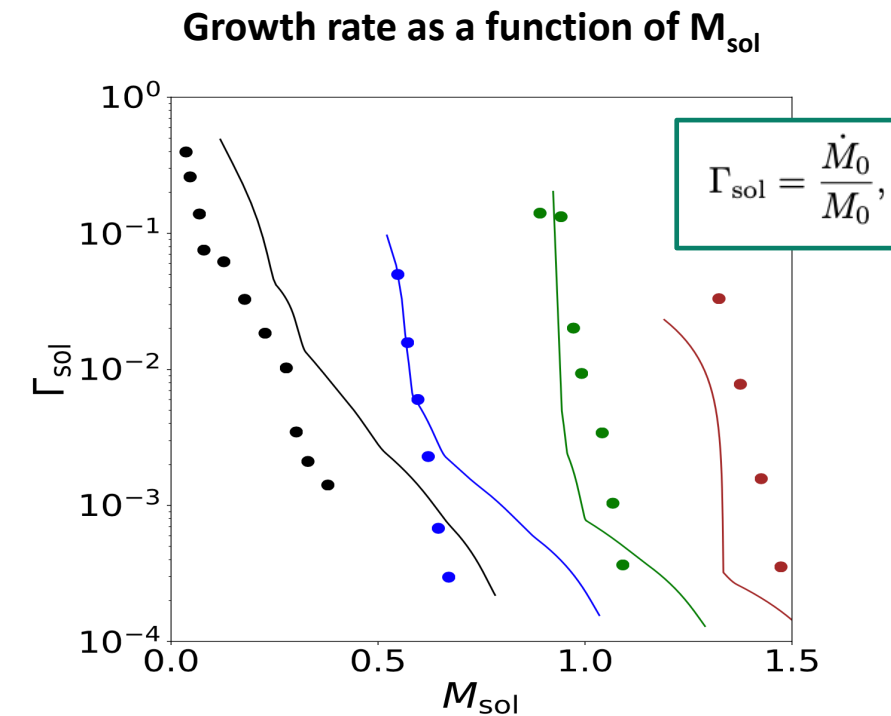
where M_c and M_h are again the core and halo masses, and $M_{\min,0} \sim 4.4 \times 10^7 (mc^2/(10^{-22} \text{ eV}))^{-3/2} M_\odot$, and the outer exponent $\alpha = 1/3$ represents the (logarithmic) slope of the relation $M_c \propto M_h^\alpha$. In order to compare with Schive et al. (2014b), we follow their definition of halo mass $M_h = (4\pi r_h^3/3)\zeta(z)\rho_{m0}$, where r_h is the halo’s virial radius, ρ_{m0} is the background matter density and $\zeta \sim 180$ (350) for $z = 0$ (≥ 1).

Previous studies were able to confirm the empirical density profile eqs. (8) and (9) using different simulations. However, they disagree about the form of the core–halo mass relation, calling the validity of eq. (11) obtained by Schive et al. (2014b) into question. Schwabe et al. (2016) performed idealised soliton merger simulations and were unable to reproduce eq. (11). Mocz et al. (2017) used a larger halo sample with simulations of a similar setup and obtained a slope of $\alpha = 5/9$, disagreeing with eq. (11). Mina et al. (2020) found the same slope of 5/9 using cosmological simulations with a box size of $2.5 \text{ Mpc } h^{-1}$. Finally, Nori & Baldi (2021) performed zoom-in simulations by including an external quantum pressure term in an N -body code, and obtained a relation with yet another value of the slope, $\alpha = 0.6$. Such disagreement between different studies indicates that there is still a fundamental lack of understanding of the core–halo structure in the FDM model, and also generates uncertainty in any constraints on the FDM mass which were obtained using eq. (11) or similar relations. Therefore, the main motivation of this work is to

Soliton growth rate for a cuspy halo

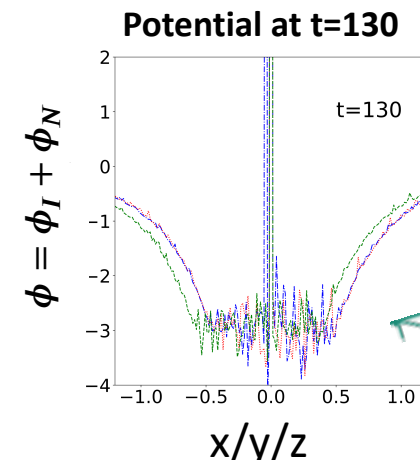
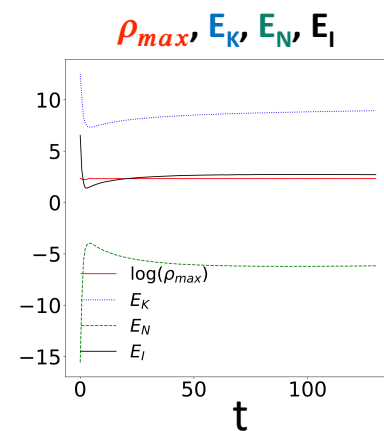
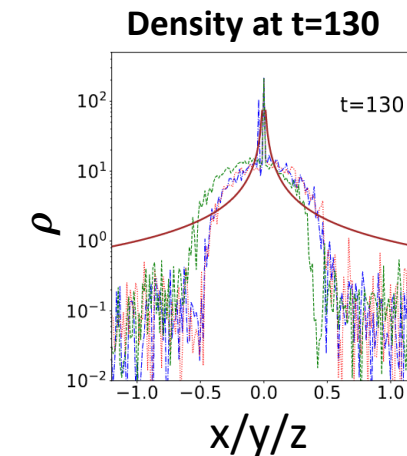
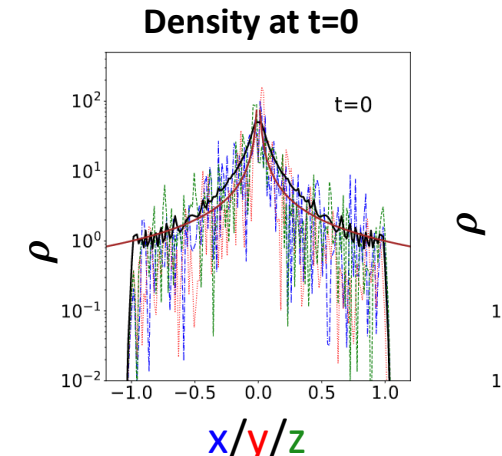
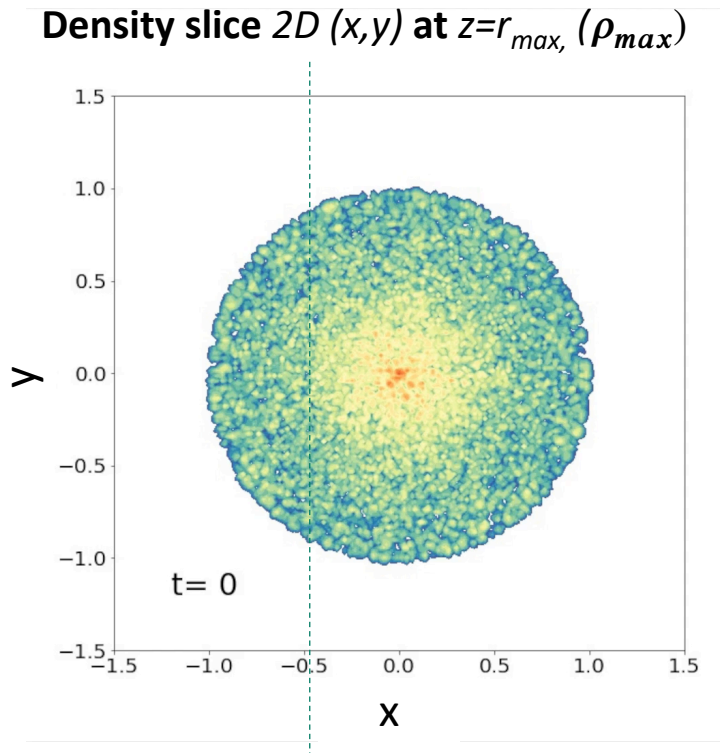


- The soliton always grows, with a growth rate that decreases with time.
- The numerical simulations suggest that the central soliton can slowly grow until it makes a large fraction of the total mass of the system, of the order of 40%.



- There is no clear sign of a scaling regime, as the growth rate still depends on the initial conditions at late times.
- Our ansatz underestimate Γ_{sol} , which remains positive but steadily decreasing in the numerical simulations.

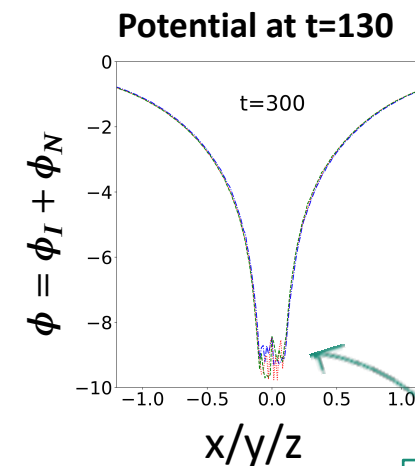
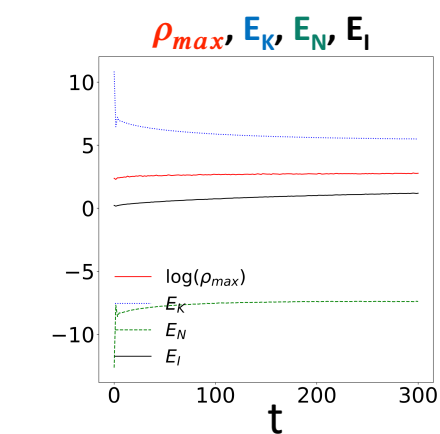
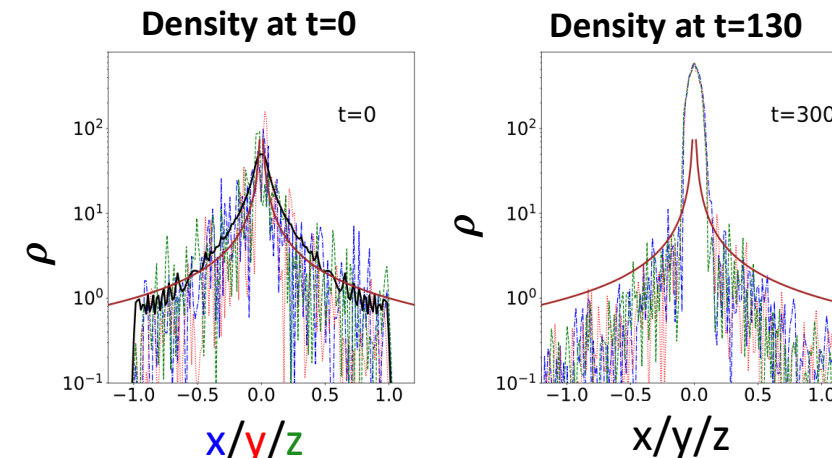
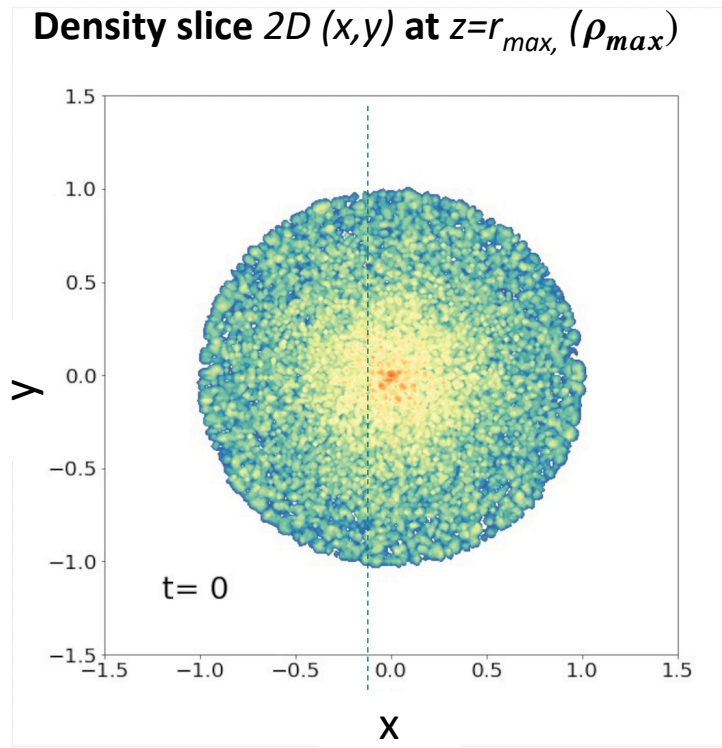
I) Cuspy halo with r_a of the order of the system



Soliton

- At $t \sim 4$, the soliton forms and contains about 33% of the total mass.
- The relaxation depletes and diffuses the halo.
- Central region: self-interacting soliton & high-density spikes far from hydrostatic eq.

I) Cuspy halo with r_a much smaller than the system



- At $t \sim 2$, formation of the central soliton
- No narrow density spikes, supported by the quantum pressure, inside this soliton.
- The hierarchy of scales: $r_a = 50 \lambda_{dB}$

Soliton

WKB

In this continuum limit, we can replace the sums in Eq.(5.24) by integrals and we obtain

$$\langle \rho_{\text{halo}}(r) \rangle = \frac{1}{2\pi^2 \epsilon^3} \int dE a(E)^2 \sqrt{2[E - \bar{\Phi}_N(r)]}, \quad (5.31)$$

where we used the WKB approximation (5.25). Comparing this expression with the classical result that expresses the density in terms of the particle phase-space distribution (Binney & Tremaine, 2008),

$$\rho_{\text{classical}}(r) = 4\pi \int_{\bar{\Phi}_N(r)}^0 dE f(E) \sqrt{2[E - \bar{\Phi}_N(r)]}, \quad (5.32)$$

where we normalized the potential so that bound orbits correspond to $E < 0$, we obtain

$$a(E)^2 = (2\pi\epsilon)^3 f(E). \quad (5.33)$$

The classical phase-space distribution can be obtained from the density by Eddington's formula (Binney & Tremaine, 2008),

$$f(E) = \frac{1}{2\sqrt{2}\pi^2} \frac{d}{dE} \int_E^0 \frac{d\Phi_N}{\sqrt{\Phi_N - E}} \frac{d\rho_{\text{classical}}}{d\Phi_N}. \quad (5.34)$$

Therefore, we look for the evolution of $M_{\text{sol}} = M_0$ and we separate the contributions of the soliton from those of the halo quasi-continuum in the sums in the right-hand side in Eq.(5.66). We also consider times much longer than the orbital periods, using

$$\lim_{t \rightarrow \infty} \frac{\sin(tx)}{x} = \pi \delta_D(x). \quad (5.67)$$

This gives

$$\begin{aligned} \dot{M}_0 = & \frac{2\pi}{\epsilon} \sum_{12} M_0^2 M_1 M_2 \left\{ \delta_D(\omega_{00}^{12}) 4V_{01;02}^2 \left(\frac{1}{M_0} - \frac{1}{M_1} \right) \right. \\ & \left. + \delta_D(\omega_0^1) \frac{V_{02;21} V_{00,01}}{M_0} \right\} + \frac{2\pi}{\epsilon} \sum_{123} M_0 M_1 M_2 M_3 \left\{ \delta_D(\omega_{01}^{23}) \right. \\ & \times \frac{1}{2} (V_{02;13} + V_{03;12})^2 \left(\frac{1}{M_0} + \frac{1}{M_1} - \frac{1}{M_2} - \frac{1}{M_3} \right) \\ & \left. + \delta_D(\omega_0^1) V_{02;21} V_{03;31} \left(\frac{1}{M_0} - \frac{1}{M_1} \right) \right\}, \end{aligned} \quad (5.68)$$

where the sums only run over the halo excited states $j \neq 0$ (and at least one is transformed into an integral in the continuum limit). Here we dropped the overbars for simplicity and we replaced \hat{V} by V as we discarded the constraints (5.58) in the sums over the halo excited states, as each of them only contains a mass of the order of ϵ^3 .